
Chapter 4
Etoposide loaded
PLGA based
nanoparticles

CHAPTER 4
FORMULATION DEVELOPMENT AND EVALUATION OF
ETOPOSIDE LOADED PLGA BASED NANOPARTICLES

4.1 Materials: Table 4.1 lists the materials obtained or purchased.

Table 4.1
List of materials

Chemical/Material	Source/Manufacturer
Etoposide	Gift sample from Biocon, Bangalore
Poly (DL lactide-co-glycolide) PLGA 50:50 (inherent viscosity 0.22 dl/g)	Gift sample from Boehringer Ingelheim Limited, Germany
Pluronic F-68 (BASF)	Gift sample from Alembic Ltd, Vadodara.
Chloroform, AR grade	SD Fine Chemicals, Mumbai
Methanol, AR grade	SD Fine Chemicals, Mumbai
Acetone, AR grade	SD Fine Chemicals, Mumbai
Potassium dihydrogen phosphate	SD Fine Chemicals, Mumbai
Disodium hydrogen phosphate	SD Fine Chemicals, Mumbai
Hydrochloric acid	SD fine Chemicals, Mumbai
Sodium hydroxide	SD fine Chemicals, Mumbai
Membrane filters, nylon (0.45 μ)	Millipore, Bangalore
Synthetic cellulose membrane (Mol. cut off value-12,000)	Himedia Labs, Mumbai
Sodium lauryl sulphate	Himedia Labs, Mumbai
Stannous octoate	Sigma, USA
Monomethoxypoly(ethyleneglycol) (mPEG, molecular weight 5000)	Sigma, St. Louis, USA
Methylene chloride	SD Fine Chemicals, Mumbai
Diethyl ether	SD Fine Chemicals, Mumbai

CHAPTER 4 A

FORMULATION DEVELOPMENT AND EVALUATION OF ETOPOSIDE LOADED PLGA NANOPARTICLES

4.2.1 Preparation of Blank PLGA Nanoparticles

Blank Nanoparticles (without the drug, Etoposide) were prepared by oil-in-water single-emulsion solvent evaporation method. (Yoo et al., 1999) using high pressure homogenization (Emulsiflex-C5, Avestin Ltd, Canada). Accurately weighed amount of PLGA was dissolved in chloroform and then poured into distilled water containing Pluronic F-68 (1% w/v) as stabilizer under continuous stirring using high speed homogenizer (Ultra-Turrax T25, IKA Labortechnik, Germany) at 8000 rpm. The dispersion was then passed through high pressure homogenizer for certain number of cycles to obtain a nanoemulsion. The organic solvent was evaporated by magnetic stirring and the nanodispersion was lyophilized (Heto Dry Winner, Denmark) to yield nanoparticles.

Three parameters were optimized in the formulation of blank nanoparticles on the basis of mean particle size (MPS). Firstly, homogenization pressure and number of homogenization cycles were optimized using a 3^2 factorial design. The two factors homogenization pressure (5000, 10000 and 15000 psi) and homogenization cycles (1, 2 and 4 cycles) were tested at three variable conditions. Total of nine batches were prepared, and each batch was prepared in triplicate.

The third parameter, ratio of volume of internal to external phase, was optimized at 1:10, 1:5, 1:4 and 1:2 ratios. In these batches, homogenization pressure and number of homogenization cycles were fixed at 10000 psi and 4 cycles respectively.

4.2.2 Formulation development of Etoposide loaded PLGA Nanoparticles

Drug loaded nanoparticles were prepared by the same method as described above. Here, Etoposide was dissolved in organic solvent (chloroform) along with PLGA and then processed as per the same procedure as described above. The nanodispersion was subjected to centrifugation at 10000 rpm for 30min (Sigma centrifuge) to remove the untrapped drug. The dispersion was finally lyophilized (Heto Dry Winner, Denmark) to yield freeze dried nanoparticles. Samples were frozen at $-70\text{ }^{\circ}\text{C}$ and placed

immediately in the freeze-drying chamber. Trehalose and sucrose were used as cryoprotectants in four concentrations 10, 20, 50 and 100% w/w of the total solid content. Effect of cryoprotectant on mean particle size was taken into consideration for optimization. For checking redispersibility, manual shaking method was used as it is clinically applicable (Freitas and Muller, 1998). Here, a weighed quantity of lyophilized NP (100mg) was taken in a test tube containing 5ml of phosphate buffer saline pH 7.4 and it was gently shaken for two minutes and the nanosuspension was subjected to particle size measurement using Malvern zetasizer. Particle in the range of more than 1micron were said to non dispersible. Drug:polymer ratio and surfactant concentration were optimized using a factorial design (explained in section 4.3) on the basis of mean particle size and entrapment efficiency.

4.3 Optimization by factorial design

Factorial design allows for the determination of the influence of the factors investigated and their interactions requiring a minimum of experiments (Box et al., 1978). Most of the experiments involve study of effects of two or more factors; in such cases factorial designs are most efficient in studying the joint effect of the factors on a response. In a factorial design, all combinations of the levels of the factors are investigated. Moreover, the design gives explanation of the responses as a function of the parameters investigated. Vandervoort and Ludwig (2002) have studied factorial design for the preparation of PLGA Nanoparticles.

A 3^2 factorial design was used in formulation Blank PLGA nanoparticles to determine the effect of two independent variables; Homogenization pressure (X1) and No. of homogenization cycles (X2) on mean particle size (MPS) (Y1, response variables). Each factor was tested at three levels designated as -1, 0 and +1.

Similarly, a 3^2 factorial design was used in formulation of ETO loaded PLGA nanoparticles to determine the effect of two independent variables; drug: polymer ratio (X3) and concentration of surfactant (X4) on entrapment efficiency (%EE) and mean particle size (MPS) (Y2 and Y3, response variables). Each factor was tested at three levels designated as -1, 0 and +1.

Table 4.2 summarizes the 9 experimental runs studied, their factor combinations, and the translation of the coded levels to the experimental units employed during the study.

Table 4.2
Factor combinations as per 3² factorial design

Batch No.	Coded factor levels	
	Factor 1(X ₁)	Factor 2(X ₂)
1	-1	-1
2	-1	0
3	-1	1
4	0	-1
5	0	0
6	0	1
7	1	-1
8	1	0
9	1	1

Translation of coded levels in actual units			
Coded level	-1	0	+1
Blank PLGA nanoparticles			
X ₁ : Homogenization pressure	5000	10000	15000
X ₂ : No. of homogenization cycles	1	2	4
ETO PLGA nanoparticles			
X ₁ : Drug: Polymer ratio	1:10	1:6	1:4
X ₂ : Surfactant Concentration (%)	0.5	1.0	1.5

The values of the factors were transformed to allow easy calculation of co-efficient in polynomial equation. To identify the effect of significant variables, the reduced model was generated. Interactive multiple regression analysis and F- statistics was utilized in order to evaluate the response. The regression equations for the two responses were calculated using equations 4.1 and 4.2.

$$\text{Response: } Y1 \text{ (MPS)} = b_0 + b_1X1 + b_2X2 + b_3X1^2 + b_4X2^2 + b_5X1X2 \quad (4.1)$$

$$\text{Response: } Y2 \text{ (\% EE)} = b_0 + b_1X1 + b_2X2 + b_3X1^2 + b_4X2^2 + b_5X1X2 \quad (4.2)$$

$$\text{Response: } Y3 \text{ (MPS)} = b_0 + b_1X1 + b_2X2 + b_3X1^2 + b_4X2^2 + b_5X1X2 \quad (4.3)$$

Where Y1 is mean particle size. Y2 and Y3 are % entrapment efficiency and mean particle size respectively. The responses in the above equation Y2 and Y3 are the quantitative effect of the formulation components or independent variables X1 and X2, which represent the drug: polymer ratio and polymer concentration of surfactant respectively; b is the coefficient of the term X.

The multiple regression was applied using Microsoft excel in order to deduce the factors having significant effect on the formulation properties. To identify the significant variables, the variables having p value > 0.05 in the full model were discarded and then the reduced model was generated for both the independent variables and each type of formulation.

In this mathematical approach, each experimental response (Y) can be represented by a quadratic equation of the response surface. Y is the measured response and b is the estimated coefficient for the factor X. The coefficients corresponding linear effects (X1 and X2), interaction (X1 X2), and the quadratic effects (X1² and X2²) were determined from the results of experiments.

Contour plots and surface response plots are diagrammatic representation of the values of the response. They are helpful in explaining the relationship between independent and dependent variables. Response surface methodology (RSM) shows relationship between an experimental response and a set of input variables. RSM sets a mathematical trend in the experimental design for determining the optimum level of experimental factors required for a given response (McCarron et al., 1999). The reduced models were used to plot two dimension contour plots and three dimension RSM using STATISTICA software at the values of X1 and X2 between -1 and +1 at predetermined value of particle size and %EE.

4.4 Evaluation of Nanoparticles

4.4.1 Particle Size and Polydispersity index

The freeze dried nanoparticles were dispersed in distilled water for particle size analysis using Malvern Zetasizer 3000 (Malvern Instruments, UK). The measurement of nanoparticle size was based on photon correlation spectroscopy (PCS). Polydispersity index was studied to determine the narrowness of the particle size distribution. All the measurements were carried out in triplicate.

4.4.2 Entrapment Efficiency

The entrapment efficiency is defined as the ratio of the amount of the encapsulated drug to that of the drug used for nanoparticles preparation. The amount of drug entrapped in NP was estimated using UV-Spectrophotometer (Shimadzu 1601UV-Visible) at 286 nm. The nanoparticle suspension in PBS was subjected to centrifugation at 10,000 rpm for 15 min and the sediment was dissolved in chloroform, diluted appropriately with chloroform and absorbance was recorded against a suitably prepared blank. The amount of unentrapped drug in the supernatant was determined by UV-Spectrophotometer at 286 nm by using PBS as blank.

4.4.3 Surface charge

Zeta potential was studied to determine the surface charge on the nanoparticles using Malvern Zetasizer 3000, (Malvern Instruments, UK). The zeta potential of the nanoparticles was determined using electrophoretic light scattering (ELS). Freeze-dried samples were resuspended in distilled water and their zeta potential was determined. All the measurements were carried out in triplicate.

4.4.4 DSC Thermograms

Thermograms were taken for Etoposide, PLGA, ETO loaded NP on a Differential Scanning Calorimeter (Mettler-Toledo, Switzerland) at a heating rate of 10°C/min in nitrogen atmosphere.

4.4.5 XRD Studies

The XRD patterns of Etoposide, Physical mixture (PLGA and ETO) and ETO loaded PLGA NP were measured with Philips PW 1729 X-ray diffractometer (Philips, Holland) using an online recorder. The instrument was operated over the 2θ range from 10° to 80° .

4.4.6 Scanning Electron Microscopy

The freeze dried nanoparticles were fastened onto a brass stub with double-sided adhesive tape. The stub was fixed into a sample holder and placed in the vacuum chamber of a JEOL JSM 1560 LV (JEOL, Tokyo, Japan) Scanning Electron Microscope and observed under low vacuum (1023 mm HG).

4.4.7 In Vitro Drug Release Studies

The in vitro drug release studies were performed using the dialysis bag diffusion technique (Leo et al., 2004). Nanoparticles corresponding to 10 mg of etoposide were placed in a dialysis bag with a MWCO of 12,000–14,000 D (Himedia, India) tied at both ends and placed in 200 ml of methanolic phosphate buffer saline (PBS) (7:3 ratio of PBS : Methanol) maintained at 37°C with continuous magnetic stirring in a beaker. At predetermined time intervals, aliquots were withdrawn from the acceptor compartment and replaced by the same volume of methanolic phosphate buffer saline. The drug content of the sample was determined by UV spectrophotometer at 286 nm after appropriate dilution with methanolic PBS. Each test was carried out in triplicate and cumulative percentage drug release was calculated. The data was statistically analyzed using the software Sigmastat (Sigma Stat, USA).

4.4.8 Mathematical modeling of drug release kinetics

Data obtained from *in vitro* release studies were fitted to various kinetic equations to understand the mechanism of drug release from formulated nanoparticles. The kinetic models used were zero order, first order, Higuchi and Peppas equation. The following plots were plotted: Q_t vs. t (zero order kinetic model); $\log(Q_0 - Q_t)$ vs. t (first order kinetic model,) and Q_t vs. square root of t (Higuchi model) and $\log M_t/M_\infty = n \log t + k$ (Peppas equation). Where Q_t is the amount of drug released at time t and Q_0 is the initial amount of drug present (Korsmeyer et al, 1983). M_t/M_∞ is the fraction of drug released after time

t in respect to amount of drug released at infinite time, k is the rate constant and n is the diffusional exponent which characterizes the transport mechanism (Peppas, 1985). Statistical comparisons were made using one way ANOVA by using the Microsoft Excel. The level of significance was considered at $p < 0.05$

4.4.9 Stability studies

The optimized formulations were studied for their stability and their potential to withstand atmospheric/environmental changes. The freeze dried (FD) samples and aqueous dispersion (AD) were sealed in Type-I amber colored glass vials. The samples were stored at 2-8°C, 25°C and 40°C. Samples were withdrawn at 1, 2 and 3 months time interval and analyzed for mean particle size and drug content. Each study was performed in triplicate.

Results and Discussion

4.5.1 Formulation Optimization of Blank PLGA NP

The blank PLGA NPs were prepared by high pressure homogenization and were optimized by 3^2 factorial design to determine the effect of two independent variables; homogenization pressure (X1) and No. of homogenization cycles (X2) on mean particle size (MPS) (Y1, response variable). The details of the nine batches (H1 to H9) is shown in Table 4.3.

Table 4.3

Optimization of process parameters during Homogenization for Blank PLGA NP by 3^2 factorial design: Factors, their levels transformed Values and Response-MPS

Batch No.	Real value		Transformed values					Response
	Homogenization pressure (X1)	No. of Cycles (X2)	X1	X2	X1 ²	X2 ²	X1X2	MPS (nm) ± SD*
H1	5000	1	-1	-1	1	1	1	595±2.1
H2	5000	2	-1	0	1	0	0	469±3.4
H3	5000	4	-1	1	1	1	-1	363±2.6
H4	10000	1	0	-1	0	1	0	230±1.7
H5	10000	2	0	0	0	0	0	149±5.2
H6	10000	4	0	1	0	1	0	98±1.3
H7	15000	1	1	-1	1	1	-1	165±2.0
H8	15000	2	1	0	1	0	0	129±2.6
H9	15000	4	1	1	1	1	1	114±2.3

* All the tests were carried out in triplicate

It was seen that as the homogenization pressure was increased from 5000 to 10000 psi, the nanoparticle size was decreased. Similarly as the number of cycles was increased from 1 to 4, the nanoparticle size was decreased. This was because homogenization leads to the development of cavitation forces, which break down the particles to smaller ones.

But as the pressure was increased above 10000 to 15000, there was no further decrease in the particle size. This is probably due to the fact that there is an optimum pressure and homogenization time (number of homogenization cycles) till which the nanoparticles undergo decrease in size and above which the excess cavitation forces and longer time leads to the particle aggregation. At higher homogenization pressures, the kinetic energy of the system increases resulting in particle collision and thereby the coagulation of particles happen, resulting in an increased particle size. The high particle collisions also distort the surfactant film coating on the nanoparticle surface and enhance the particle aggregation thereby resulting in larger sizes (Freitas and Muller, 1998). The number of homogenization cycles was optimized to be four and homogenization pressure of 10000 psi was found to be optimum. Hence processing conditions of batch H6 were found to be optimum. Fig. 4.1 shows mean particle size distribution nanoparticles of Batch No H6

The mean particle size of NP ranged from 98 ± 1.3 to 595 ± 2.1 nm. The lowest MPS was observed in middle level of X1 (10000 psi) and highest level of X2 (4 cycles) in batch H6.

The equations for full model for Y1 (MPS) is given by equation 4.4.

$$Y1 (\text{MPS}) = 151.11 - 22.1X1 - 69.16X2 + 146.83X1^2 + 11.83X2^2 + 45.25X1X2 \quad (4.4)$$

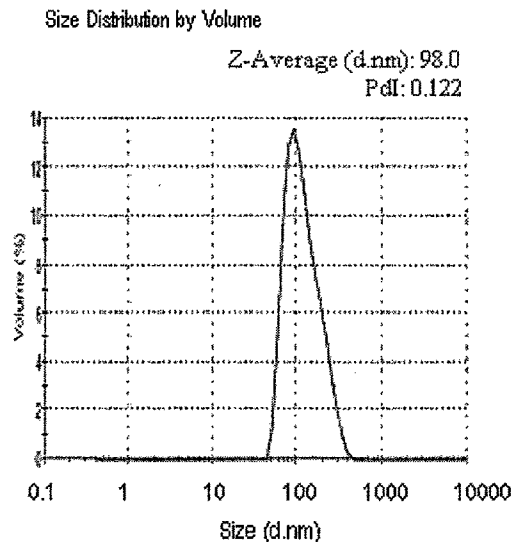


Fig. 4.1: Mean Particle Size distribution and PDI of nanoparticles of Batch No H6

Table 4.4 shows model coefficients estimated by multiple linear regression for MPS. The regression coefficients having P value < 0.05 are highly significant. There were no terms having coefficients with P value > 0.05 and hence all the terms were contributing in the prediction of mean particle size.

Table 4.4
Model coefficients estimated by multiple linear regression.

Factor	Coefficient	Coefficient calculated value	Computed t-value	P-value
Intercept	β_0	151.111	55.38731	1.3E-05
X1	β_1	-169.833	-113.652	1.5E-06
X2	β_2	-69.166	-46.286	2.22E-05
X1 ²	β_{11}	146.833	56.73059	1.21E-05
X2 ²	β_{22}	11.833	4.571931	0.019634
X1X2	β_{12}	45.25	24.72442	0.000145

Analysis of Variance (ANOVA) of Full Model for MPS is shown in Table 4.5. Model F value (3781.936) was more than tabulated F value ($F_{tab} = 9.01$) indicating that the full model was significant. The R² value is a measure of total variability explained by the model. The R² value of 0.9998 for the full model indicates that the model is significant. That means the model can explain 99.98% of variability around the mean. The R² adjusted value of the full model was also high (0.9995).

Table 4.5
Analysis of Variance (ANOVA) of full model

	DF	SS	MS	F	Significance F	R ²	Adj R ²
Regression	5	253354.69	50670.94	3781.936	6.78E-06	0.9998	0.9995
Error	3	40.194	13.39				

Table 4.6 shows each of the observed values of Y and was compared with the predicted values of Y from the model. The residual value and percent error was calculated to show the correlation between the observed and the predicted values. The low residuals values and percentage error less than 5% show significance of the model used.

Table 4.6
Observed responses and Predicted values for MPS

Batch No.	Observed value	Predicted value	Residual value	% Error
H1	595	594.027	0.972	0.667
H2	469	467.777	1.222	0.260
H3	363	365.194	-2.194	0.604
H4	230	232.111	-2.111	0.917
H5	149	151.111	-2.111	1.416
H6	98	93.777	4.222	4.308
H7	165	163.861	1.138	0.689
H8	129	128.111	0.888	0.688
H9	114	116.027	-2.027	1.778

The contour plots and the response surface curves give a diagrammatic representation of the values of the response and are shown in Fig. 4.2a and 4.2b respectively for MPS. The contour plots and response surface curves were drawn at -1 level to 1 level of X1 and X2. The plots were found to be linear; therefore linear relationship exists between X1 and X2 variables. It was concluded from the plots that the MPS of 98.26nm could be obtained with X1 range from -0.15 level (9250psi) to 1.0 level (15000psi) and X2 range from -0.3 (1.7 cycles) to 1.0 (4 cycles).

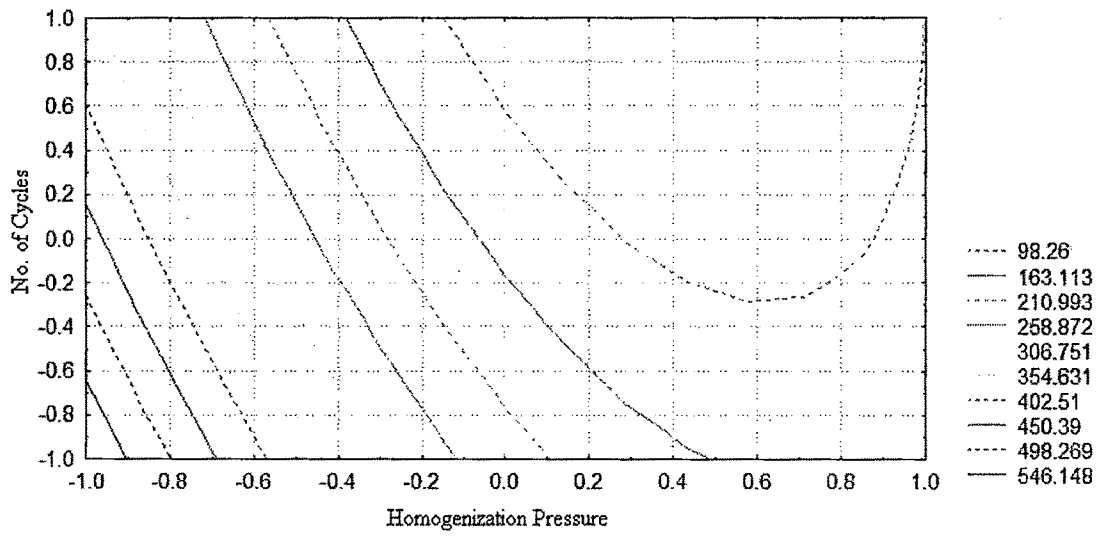


Fig. 4.2a: Contour plot for response of MPS for X1 (homogenization pressure) and X2 (no. of homogenization cycles) between -1 to 1.

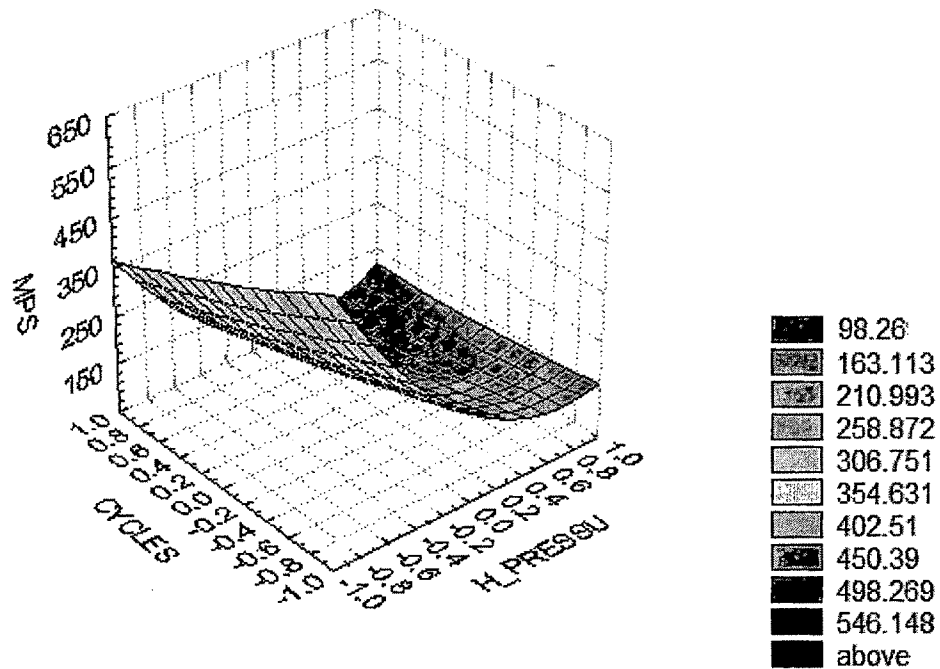


Fig. 4.2b: Response Surface Plot for response of MPS for X1 (homogenization pressure) and X2 (no. of homogenization cycles) between -1 to 1.

The other factor taken under consideration for optimization of homogenization conditions was polydispersity index (PDI). Polydispersity index is a measure of dispersion homogeneity and usually ranges from 0 to 1. Values close to 0 indicate a homogeneous dispersion while those greater than 0.3 indicate high heterogeneity (Ahlin et al, 2002). Fig. 4.3 gives a visual representation of the effect of homogenization pressure and number of homogenization cycles during homogenization on mean particle size and PDI of the formed nanoparticles of the nine batches (H1 to H9). PDI values were less than 0.3 for all batches except H1 and H2. It was concluded that Batch No. H6 had the least PDI (0.12) and was considered optimum as it also had least MPS.

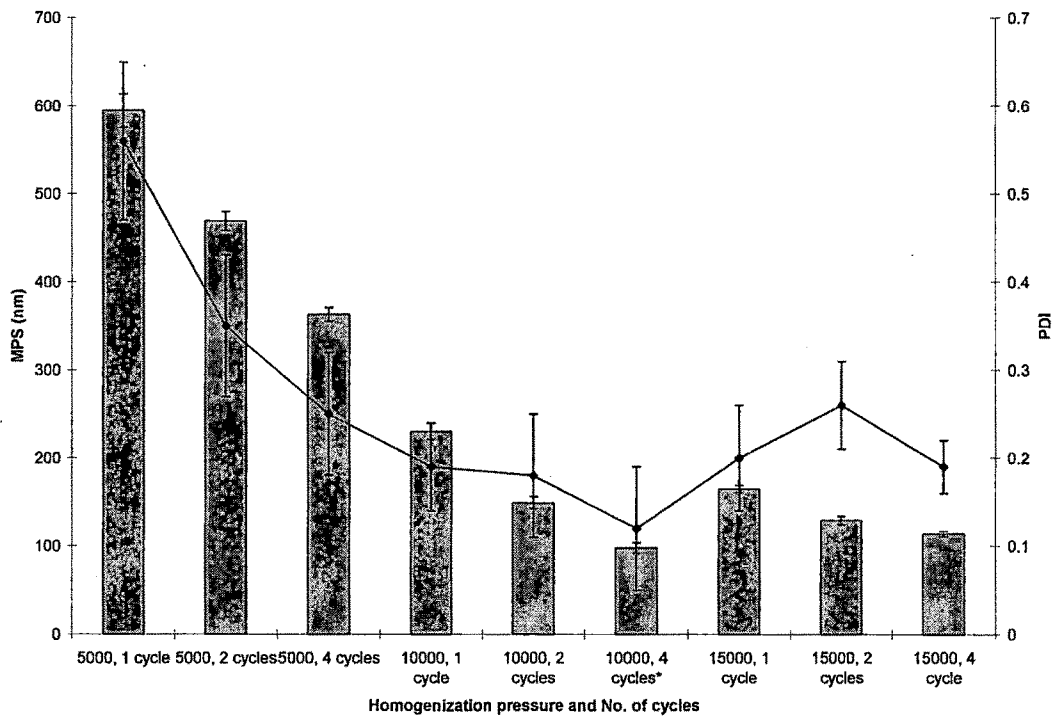


Fig. 4.3: Effect of process parameters (Homogenization pressure and Number of Homogenization cycles) during Homogenization on mean particle size and PDI of formed nanoparticles.

The third factor optimized was solvent ratio of internal phase to external phase of the oil in water emulsion. The internal phase was kept constant (5ml) and the external phase was varied from 10, 20, 25 to 50ml to give four different ratios of 1:2, 1:4 and 1:5 (Table 4.7). As the external phase volume increased from 10 to 25 ml, there was a reduction of particle size from 221 to 121nm. This size reduction may be ascribed to the reduced viscosity of the organic phase, which facilitates the solvent diffusion to water. But as the volume of the external solvent was further increased to 50 ml, there was an increase in the MPS (156 nm), probably due to the fact that the organic solvent required much more time to evaporate and particles aggregated during this stage resulting in increase in size. The PDI was least for 1: 5 ratio and even the particle size was minimum, hence the ratio of 1:5 taken as optimum for preparation of PLGA NP.

Table 4.7

Influence of ratio of volume of internal/external phase during homogenization on MPS

Ratio of volume of internal/external phase	Mean Particle size nm ±SD	PDI ±SD
1:2	221±9.71	0.26±0.012
1:4	178±11.23	0.15±0.018
1:5	121±5.65	0.05±0.008
1:10	156±12.49	0.09 ±0.023

4.5.2 Optimization using Factorial Design for formulation of Etoposide loaded PLGA NP

Nine batches were prepared as per 3^2 factorial design to study the effect of two independent variables, ratio of drug and polymer (X1), surfactant concentration (X2) on the two responses, percentage entrapment efficiency (Y1) and mean particle size (Y2) of the PLGA Nanoparticles. Table 4.8 displays the values of Factors, their levels and transformed Values and values of both the responses, %EE and MPS as per 3^2 factorial design.

Table 4.8
Formulation of ETO-PLGA NP by 3^2 factorial design:
Factors, their levels and transformed Values, Response: %EE and MPS

Batch No:	Real value		Transformed values					Response	
	Drug: Polymer ratio (mg)	Surf Conc. (% w/v)	X1	X2	X1 ²	X2 ²	X1X2	% EE ± SD*	MPS (nm) ± SD*
ENP1	1:10	0.5	-1	-1	1	1	1	79.05±3.2	182± 9.1
ENP2	1:10	1.0	-1	0	1	0	0	83.12±8.3	160± 8.2
ENP3	1:10	1.5	-1	1	1	1	-1	81.04±7.6	153± 5.6
ENP4	1:6	0.5	0	-1	0	1	0	71.45±8.2	146± 7.1
ENP5	1:6	1.0	0	0	0	0	0	77.42±4.2	112± 9.3
ENP6	1:6	1.5	0	1	0	1	0	74.20±5.3	110± 5.9
ENP7	1:4	0.5	1	-1	1	1	-1	53.72±6.2	141± 1.3
ENP8	1:4	1.0	1	0	1	0	0	54.59±4.9	116±2.1
ENP9	1:4	1.5	1	1	1	1	1	43.64±4.3	105±1.5

* All the tests were carried out in triplicate

4.5.2.1 Entrapment Efficiency

The % EE of ETO in PLGA 50:50 NP varied from 43.64±5.51% to 79.05±4.39%. The highest %EE was observed in lowest levels of X1 (1:10) and lowest level of X2 (0.5%w/v) in batch N1. The responses in the equation Y2 are the quantitative effect of the formulation components or independent variables X1 and X2. The equation 4.5 is for the full model.

$$Y2 (\%EE) = 77.37-15.21X1-0.89X2-8.49X1^2- 4.52X2^2- 3.01X1X2 \quad (4.5)$$

Table 4.9
Model coefficients estimated by multiple linear regression for EE.

Factor	Coefficient	Coefficient calculated value	Computed t- value	P-value
Intercept	β_0	77.37444	42.29239	2.91E-05
X1	β_1	-15.21	-15.1787	0.000621
X2	β_2	-0.89	-0.88817	0.439875
X1 ²	β_{11}	-8.49667	-4.89544	0.016309
X2 ²	β_{22}	-4.52667	-2.60809	0.079817
X1X2	β_{12}	-3.0175	-2.4587	0.090973

The results of the regression output and response of full model are presented in Table 4.9 and Analysis of Variance (ANOVA) of full model is presented in Table 4.10. Model F value is assessed by the F statistic, which estimates the percentage of the variability in the outcome explained by the model (Hocking RR. 1976). Model F value (53.598) for this was more than the tabulated F value ($F_{tab} = 9.01$), implying that the model was significant. The R² value of the full model was also high (0.98893). The R² value explains variability around the mean, therefore the model was able to explain 98.89% variability in the results. The regression coefficients having P value < 0.05 are highly significant. The terms having coefficients with P value > 0.05 were removed from the model to give the

reduced model equation. However, in our case, omitting the terms with P value >0.05 resulted in a reduced model with decreased adjusted R² values (Table 4.9). Adjusted R² improves when non significant terms are eliminated from full model equation, but in our case it didn't happen. Since the adjusted R² value did not improve, the reduced model was not sought and a reduced model was not developed in this case.

Table 4.10
Analysis of Variance (ANOVA) of Full and Reduced Model for EE

	Full model		Reduced model	
	Regression	Error	Regression	Error
DF	5	3	2	6
SS	1614.606	18.07441	1532.4512	100.22966
MS	322.921	6.02480	766.225	16.7049
F	53.598		45.8681	
Significance F	0.003915		0.00023	
R ²	0.98893		0.93861	
Adj R ²	0.970479		0.918147	

The results show that % EE greatly depend on the drug polymer ratio. Increase in drug polymer ratio from 1:4 to 1:10 increased the %EE. The concentration of the surfactant did not have significant effect on the EE as the P value obtained was more than 0.05 in all the X₂ terms.

Table 4.11 shows each of the observed values of Y and was compared with the predicted values of Y from the model. The residual value and percent error was calculated to show the correlation between the observed and the predicted values. The low residuals values and percentage error less than 5% show significance of the model used.

Table 4.11
Observed responses and Predicted values for EE

Batch No.	Observed value	Predicted value	Residual value	% Error
ENP1	79.05	77.433	1.616	1.500
ENP2	83.12	84.087	-0.967	1.499
ENP3	81.04	81.688	-0.648	0.793
ENP4	71.45	73.737	-2.287	2.893
ENP5	77.42	77.374	0.0455	0.058
ENP6	74.2	71.957	2.242	3.116
ENP7	53.72	53.048	0.671	1.264
ENP8	54.59	53.667	0.922	1.718
ENP9	43.64	45.233	-1.593	3.521

The visual picture of the output by the two dimensional contour plots and three dimensional response surface plots are shown in Fig. 4.4a and Fig 4.4b respectively. The plots were found to be non-linear; therefore non-linear relationship existed between X1 and X2 variables. Moreover, X2 variable (surfactant concentration) did not have significant effect on the response EE. It was seen from the plots that X2 range was wide from -1 to 1 for obtaining the EE responses (except for EE of 80%). It was concluded from the contour and surface plots that the % EE of 80% could be achieved with X1 range from -1.2 to -0.5 level and X2 range at -0.6 level to 1.2 level.

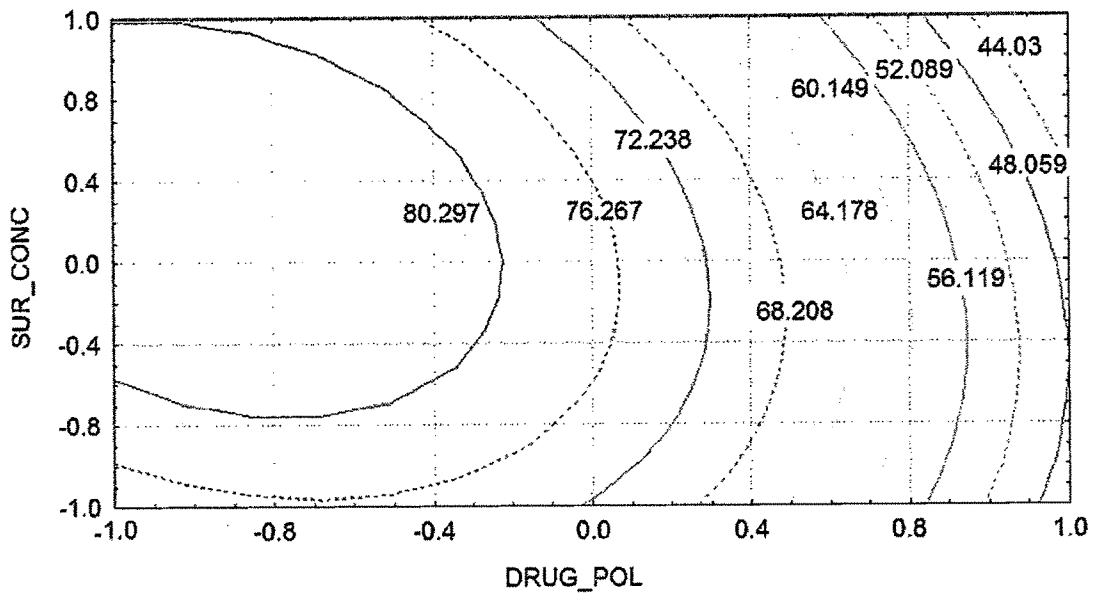


Fig. 4.4a: Contour plot of EE of ETO-PLGA NP

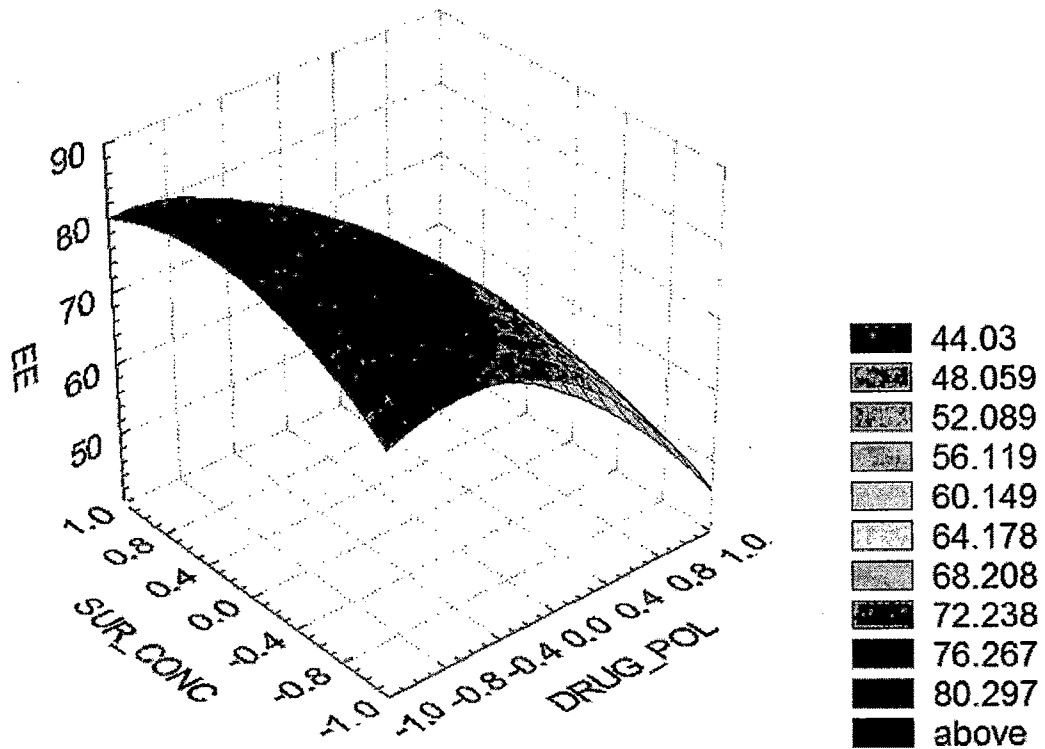


Fig. 4.4b: Surface Response of EE of ETO-PLGA NP

4.5.2.2 Mean Particle Size

The mean particle size of NP ranged from 105±5.4 to 182±5.5 nm. The lowest MPS was observed in highest level of X1 (1:4) and highest level of X2 (1.5%w/v) in batch N1.

The full model for Y2 (MPS) is given by equation 4.6.

$$Y2 \text{ (MPS)} = 115.88 - 22.1X1 - 16.833X2 + 20.16X1^2 + 10.16X2^2 - 1.75X1X2 \quad (4.6)$$

Table 4.12 shows model coefficients estimated by multiple linear regression for MPS. The regression coefficients having P value < 0.05 are highly significant. The terms having coefficients with P value > 0.05 are least contributing in the prediction of mean particle size and hence the factor X1X2 having P value > 0.05 was removed from the full model to give the reduced model equation.

The equation 4.7 explains the reduced model for Y2 (MPS).

$$Y2 \text{ (MPS)} = 115.88 - 22.1X1 - 16.833X2 + 20.16X1^2 + 10.16X2^2 \quad (4.7)$$

Summary of regression results for MPS for both Full model and Reduced model is shown in table 4.12

Table 4.12
Model Coefficients Estimated By Multiple Linear Regression For MPS

Factor	Full model			Reduced model		
	Coefficient value	Computed t-value	P-value	Coefficient value	Computed t-value	P-value
Intercept	115.8889	43.57512	2.66E-05	115.8889	43.78258	1.63E-06
X1	-22.1667	-15.2173	0.000616	-22.1667	-15.2897	0.000107
X2	-16.8333	-11.556	0.001391	-16.8333	-11.611	0.000314
X1 ²	20.16667	7.992997	0.004087	20.16667	8.031052	0.001305
X2 ²	10.16667	4.029527	0.027474	10.16667	4.048712	0.015492
X1X2	-1.75	-0.98091	0.398972			

Analysis of Variance (ANOVA) of Full and Reduced Model for MPS is shown in Table 4.13. Model F value of 89.23855 implies that the full model is significant ($F_{\text{tab}} = 9.01$). Model F value of the reduced model is 112.37 and the F_{tab} value is 6.39, showing that the model is significant.

Table 4.13
Analysis of Variance (ANOVA) of Full and Reduced Model for MPS

	Full model		Reduced model	
	Regression	Error	Regression	Error
DF	5	3	4	4
SS	5680.694	38.19444	5668.444	50.44444
MS	1136.139	12.73148	1417.111	12.61111
F	89.23855		112.37	
Significance f	0.001842		0.000232	
R ²	0.993321		0.991179	
Adj R ²	0.98219		0.982359	

The R² value is a measure of total variability explained by the model. The R² value of 0.993321 for the full model indicates that the model is significant. That means the model can explain 99.33% of variability around the mean. R² of the reduced model is 0.991179, which is also high but lower than the full model because as the number of factors are added to the model (even if these factors are not significant), the R² value increase (Montgomery DC, 2004). This explains the higher R² value of the full model than the reduced model. In such cases the term R² adjusted has to be checked. It is called adjusted as the value has been adjusted for the size of the model. The R² adjusted decreases when non significant terms are added to the equation. Removal of non significant terms improves the value of R² adjusted as evident from the value of R² adjusted in the reduced model which is 0.982359 and is greater than the R² adjusted value of the full model (0.98219).

Table 4.14 shows each of the observed values of Y and was compared with the predicted values of Y from the model. The residual value and percent error was calculated to show the correlation between the observed and the predicted values. The low residuals values and percentage error less than 5% show significance of the model used.

Table 4.14
Observed Responses and Predicted Values for Full and Reduced Model MPS

Batch No.	Observed value	FULL MODEL			REDUCED MODEL		
		Predicted value	Residual value	% Error	Predicted value	Residual value	% Error
ENP1	182	183.472	-1.472	0.801	185.222	-3.222	1.738
ENP2	160	158.222	1.777	1.118	158.222	1.777	1.118
ENP3	153	153.305	-0.305	0.198	151.555	1.444	0.905
ENP4	146	142.888	3.111	2.176	142.888	3.111	2.176
ENP5	112	115.888	-3.888	3.348	115.888	-3.888	3.348
ENP6	110	109.222	0.777	0.711	109.222	0.777	0.711
ENP7	141	142.638	-1.638	1.148	140.888	0.111	0.078
ENP8	116	113.888	2.111	1.852	113.888	2.111	1.852
ENP9	105	105.472	-0.472	0.447	107.222	-2.222	2.070

The contour plots and the response surface curves were drawn at -1 level to 1 level of X1 and X2 to give a diagrammatic representation of the values of the response and are shown in Fig. 4.5a and 4.5b respectively for MPS. The plots were found to be linear; therefore linear relationship exists between X1 and X2 variables. It was concluded from the contour and the response surface curves that the MPS of 109 nm could be obtained with X1 range from -1 level (1:10) to 0.0 level (1:6) and X2 range from 0.2 (1.25%) to 1.0 (1.5).

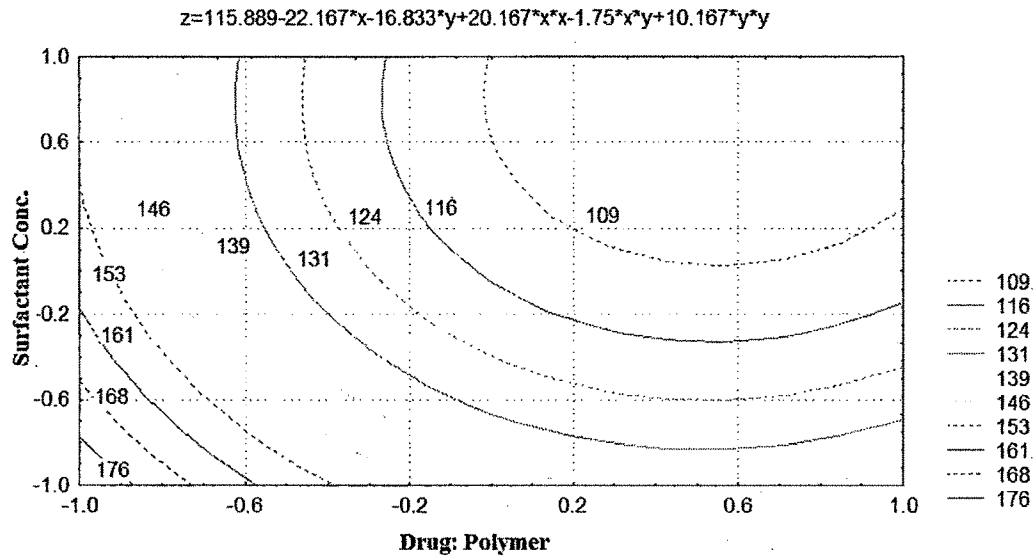


Fig. 4.5a: Contour plot for MPS of ETO-PLGA NP

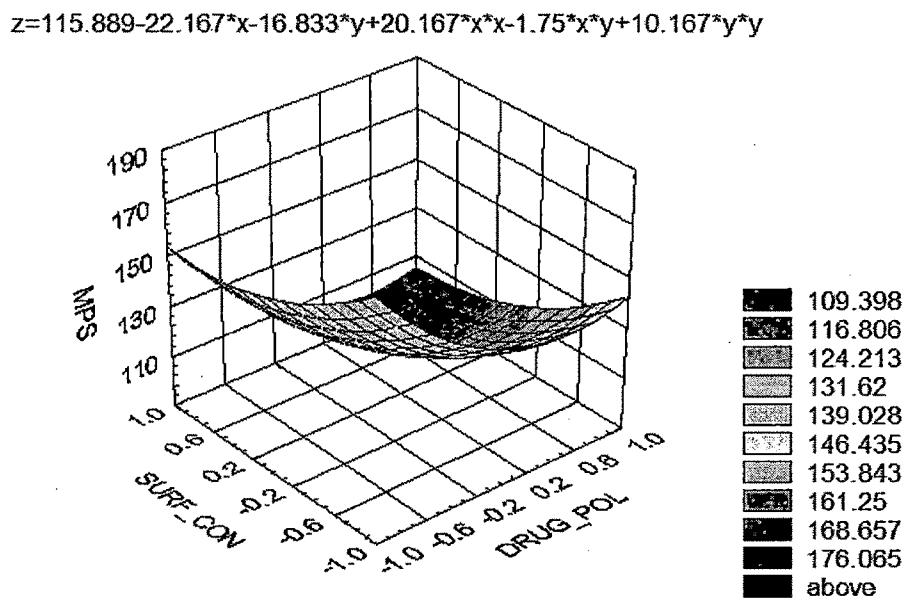


Fig. 4.5b: Surface Response of MPS of ETO-PLGA NP

4.5.2.3 Check point analysis:

To check the adequacy of the above regression model, a check point analysis was carried out taking intermediate levels of the formulation variables. Table 4.15a shows the actual and coded values. The actual concentration of drug and polymer ratio taken was 1:5 and surfactant concentration taken was 0.75%.

The coded levels were calculated for both the factors by using the formula

$$\text{Coded level} = \frac{\text{actual value} - (\text{lowest value} + \text{highest value}) / 2}{(\text{Highest value} - \text{lowest value}) / 2}$$

Table 4.15a
Actual level and coded level for check point analysis

Factor	Actual level	coded level
Drug: polymer ratio	1:5	+0.33
Surfactant Concentration	0.75	-0.5

Table 4.15b
Regression analysis of check point analysis

Factor level	predicted MPS	Experimental MPS	t calculated	t tabulated
Drug: polymer (1:5)	121.738	125	-0.07897	3.18244
Surfactant Concentration (0.75%)		128		
		115		
		118		

From the regression equation and the surface response curve, the predicted values of the response (Mean particle size) were obtained (Table 4.15b).

A set of four experimental runs were undertaken (Table 4.15b) to determine the Mean Particle Size of the drug loaded Nanoparticles at the above mentioned levels (drug polymer ratio of 1:5; surfactant concentration of 0.75%). The mean responses were calculated and the values of predicted and actual response are shown in Table 4.15.

The predicted and actual responses were compared by student's t test. Since the calculated t value is less than the tabulated value, we can conclude that there is no significant difference between the values. The P value for two tailed test at 95% confidence level is 0.94 which is greater than 0.05 indicating non significant difference in the results of the predicted and experimental values of MPS.

4.5.3 Zeta potential

Zeta potential is the potential at the hydrodynamic shear plane and can be determined from the particle mobility under an applied electric field. The mobility will depend on the effective charge on the surface. Zeta potential is also a function of electrolyte concentration. Kesisoglou et al. (2007) explained in their review that Surface charge on the nanoparticle arises due to (i) ionization of the particle surface or (ii) adsorption of ions (such as surfactants) onto the surface. Zeta potential gives information to predict the storage stability of colloidal dispersions (Thode et al., 2000). In general, the greater the zeta potential value of a nanoparticulate system, the better the colloidal suspension stability due to repulsion effect between charged nanoparticles. The zeta potential values ranged between -23.0 to -34.2mV. It was evident from the Table 4.16 that the surfactant concentration affected the charge on the particle. It was seen that as the surfactant concentration was increased from 0.5 to 1.5%, there was a decrease in the zeta potential value. This is because the surfactant is non- ionic and increasing its concentration lowers the total charge on the particle. The optimized batch of ETO loaded PLGA nanoparticle (ENP5) was found to have Zeta potential of -32.7 ± 1.68 mV. Zeta potential values in the -15 mV to -30 mV are common for well-stabilized nanoparticles (Kesisoglou et al., 2007). Figure 4.6 shows Zeta potential distribution of batch no ENP9.

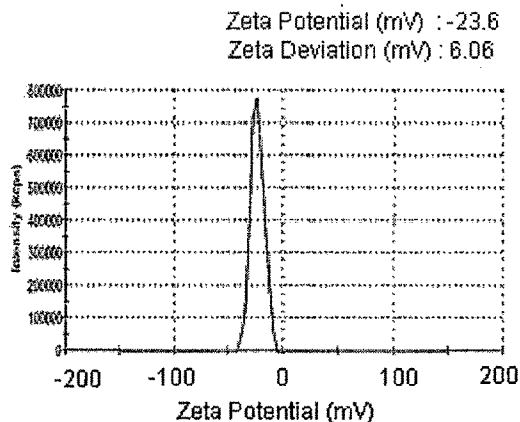


Fig 4.6: Zeta potential distribution of ETO loaded PLGA nanoparticle batch no ENP5

Table 4.16
Influence of Surfactant Concentration and drug loading on zeta potential

Batch No.	Drug :Polymer Ratio	Drug loading (%)	Surf Conc. (% w/v)	Zeta Potential (mV)
ENP1	1:10	9	0.5	-30.8
ENP2	1:10	9	1.0	-29.6
ENP3	1:10	9	1.5	-27.0
ENP4	1:6	14	0.5	-34.2
ENP5	1:6	14	1.0	-32.2
ENP6	1:6	14	1.5	-29.5
ENP7	1:4	20	0.5	-31.0
ENP8	1:4	20	1.0	-27.3
ENP9	1:4	20	1.5	-23.0

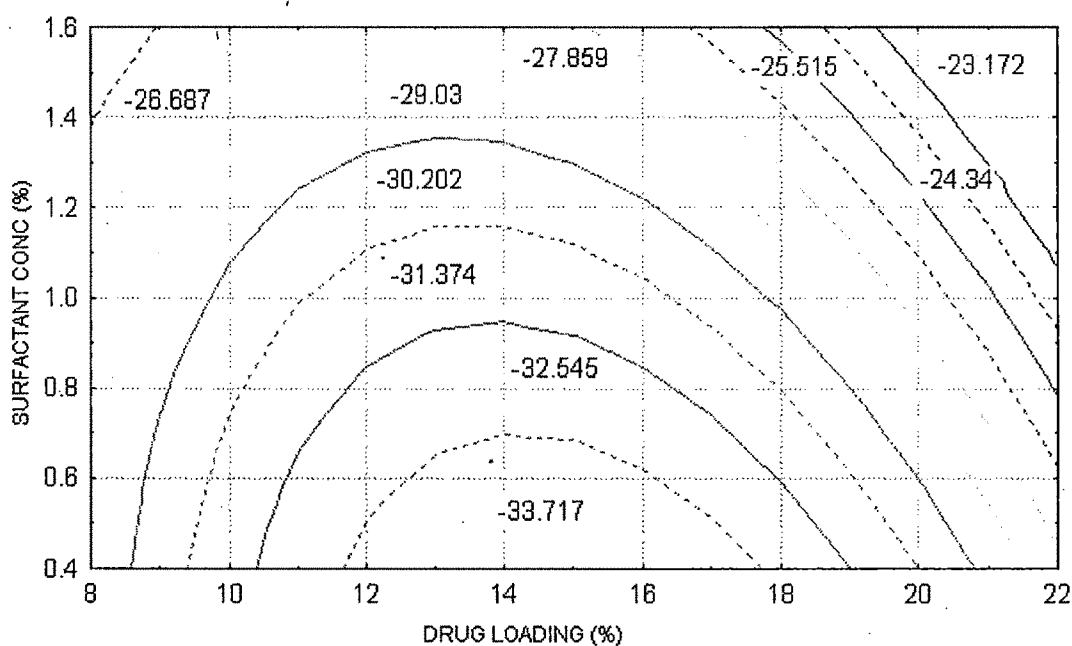


Fig 4.7: Contour plot showing Zeta potential values: Combined Effect of Surfactant Concentration and drug loading

A contour plot was drawn from the values obtained from Table 4.16 to study the combined effect of surfactant concentration and drug loading (polymer was kept constant in all batches) on zeta potential. From the contour plot in Fig. 4.7 it was seen that a high negative zeta potential of -33.71mV could be obtained by using surfactant concentration in the range of 0.4 to 0.7% and drug loading of 11.8 to 17.8%.

Effect of pH on Zeta potential of PLGA NP

The surface charge on the nanoparticles is said to vary as per the pH of the dispersion medium (Panyam et al., 2002). Hence we used different pH of the dispersion medium from 2.0 to 7.4 and checked the zeta potential of the nanoparticles at the particular pH of the medium. Fig 4.8 shows the effect of change in the pH of the dispersion medium on the surface charge of the nanoparticles.

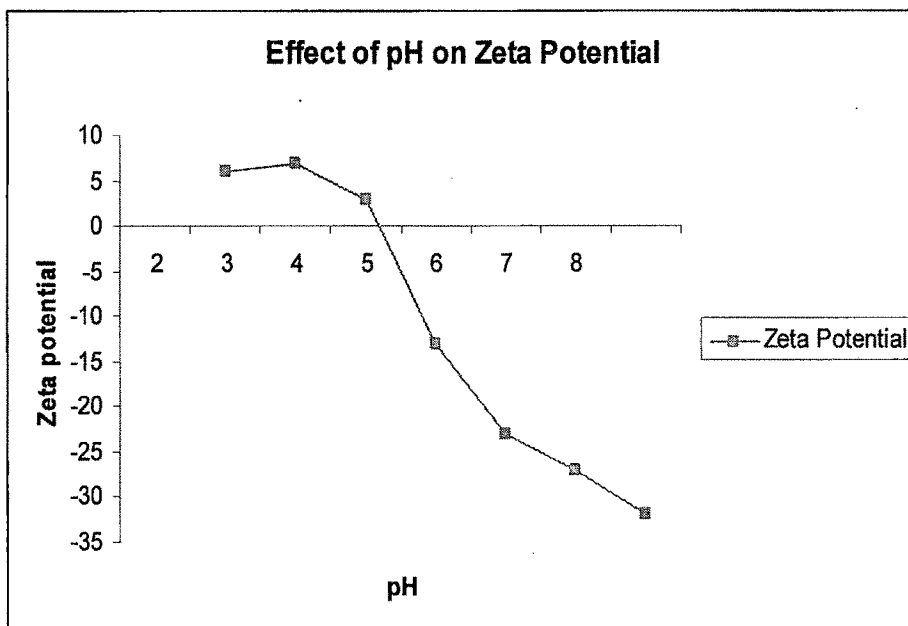


Fig. 4.8: Influence of pH on zeta potential

It has been reported that there is a rapid reversal of surface charge of NPs from anionic to cationic in the endolysosomal compartment and in this process the NPs would escape into the cytosol (Panyam et al., 2002). It was seen from the Fig. 4.8 that when the dispersion medium was alkaline, the charge was negative and when the medium was acidic, the charge became positive. Therefore when such particles would enter in the acidic environment (present in endolysosomal compartment) of the cells, there would occur a rapid reversal of surface charge of NPs from anionic to cationic. In this process, the NPs would escape into the cytosol, which would prevent their degradation in the cell. Hence the NPs would not degrade in the cells.

4.5.4 Optimization of cryoprotectant

Lyophilization is the process in which freeze-drying is done to remove solvent from the formulation and the formulation is transformed into a solid dosage form. Freeze drying increases stability of the formulation as the solvent is removed. The presence of water accelerates degradation of various types of polymers used in NPs (Chacon et al., 1999). Schaffazick et al have shown that freeze-drying is a safe process as it does not interfere with the structural integrity of the nanoparticle and also does not cause leakage of drug (Schaffazick et al 2003). A cryoprotectant (e.g., trehalose, sorbitol, mannose, and glucose) is added to the dispersion before lyophilizing. Chacon et al. reported that sugars ensure a readily dispersible powder and also improves stability of PLGA NPs with freeze-drying (Chacon et al., 1999). Trehalose too has been reported as cryoprotectant in PLGA based NPs and has shown good redispersibility (Ahlin et al., 2002). In the present study we used sucrose and trehalose as cryoprotectants in the concentration of 10, 20, 50 and 100% w/w of the solid mass.

Table 4.17 indicates the different concentrations of the two cryoprotectants used and their effect on particle size after lyophilization. An increase in size of the NPs was seen following freeze-drying with the aid of both the cryoprotectants sucrose and trehalose. The increase in size of NP after freeze drying has been reported (Saez et al., 2000).

It was seen that sucrose in 20% w/w concentration shows least increase in particle size and had good redispersibility. Mean particle size of with Trehlose at 50% concentration showed least increase in MPS, but it didn't have good redispersibility. Hence sucrose in 20%w/w concentration was found to be optimum for lyophilization with least increase in MPS and good redispersibility.

Table 4.17

Optimization of Cryoprotectant : Influence of lyophilization on particle size and redispersibility

Cryoprotectant	% w/w	Mean Particle Size (nm) Before Lyophilization	Mean Particle Size (nm) After Lyophilization	Redispersibility
No Cryoprotectant	0	119	121	ND
Sucrose	10	119	119	ND
Sucrose	20	119	124	D
Sucrose	50	119	126	D
Sucrose	100	119	130	D
Trehalose	10	119	120	ND
Trehalose	20	119	126	ND
Trehalose	50	119	130	ND
Trehalose	100	119	139	D

D- dispersible, ND- non dispersible.

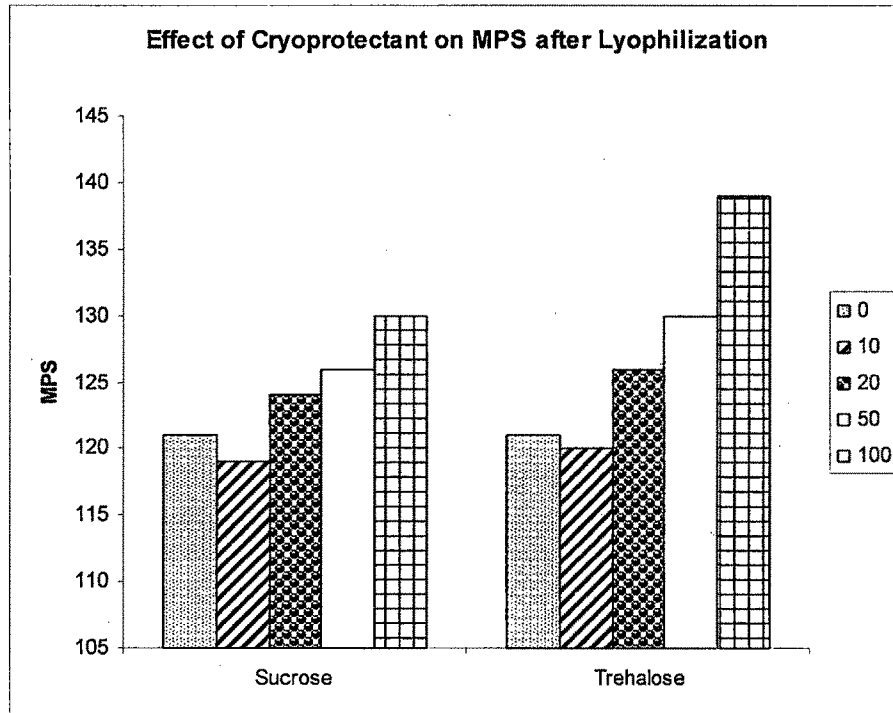


Fig. 4.9: Effect of Cryoprotectant on MPS after Lyophilization

4.5.5 DSC studies

Differential Scanning Calorimetry (DSC) gives information regarding the physical properties like crystalline or amorphous nature of the samples (Sophie-Dorothee et al., 1999). The DSC thermograms (Fig. 4.10) of etoposide, PLGA, etoposide loaded NP depicted endothermic peaks. Etoposide showed endothermic peak was at 185.26 °C, PLGA had peak at 54.11 °C and ENP5 had peak at 57.81 °C. When the endothermic curves of the drug are not visible in the nanoparticle formulation, it is said to be in an amorphous state in the nanoparticles (Mandal et al., 2002). Hence it was concluded that in the prepared PLGA NP, the drug was present in the amorphous phase and may have been homogeneously dispersed in the PLGA matrix.

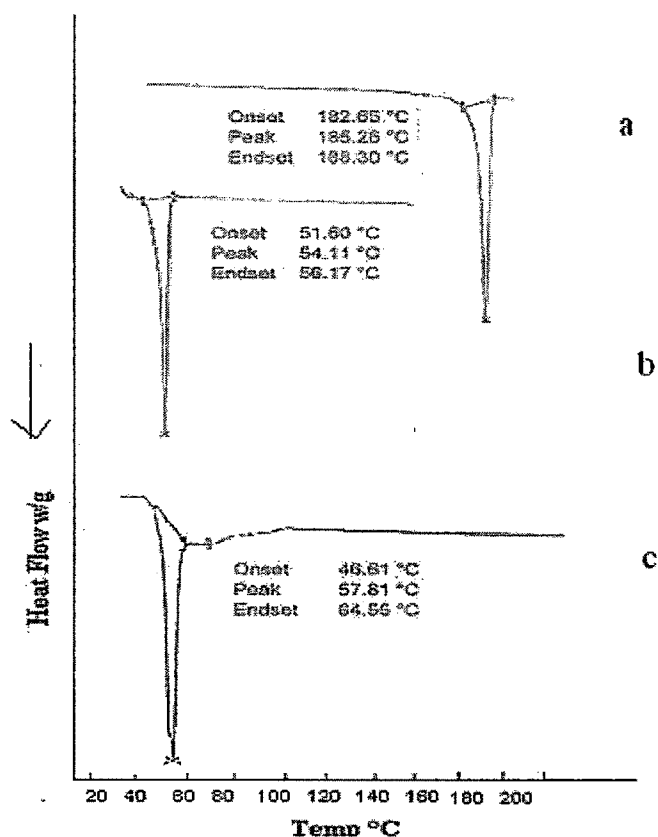


Fig. 4.10: DSC thermogram of (a)Etoposide, (b)PLGA and (c)Etoposide loaded Nanoparticles (ENP5)

4.5.6 XRD studies

Fig. 4.11 shows the X-ray diffraction scans of pure drug etoposide (ETO), physical mixture of ETO and PLGA (PM) and ETO-loaded PLGA nanoparticles (ETO-PLGA NP). ETO showed four principle peaks at 23° (1400 counts), 19° (1300 counts), 17° (900 counts) and 24° (700 counts). In the physical mixture, four peaks were visible at 23° (500 counts), 22° (350 counts), 19° (375 counts) and 16° (270 counts), though their intensities were reduced. It was observed that these characteristic peaks disappeared in ETO-entrapped nanoparticles (ETO-PLGA NP). It was concluded that ETO existed in the amorphous state in the polymeric nanoparticles and there was no presence of crystalline drug on the surface of the NPs.

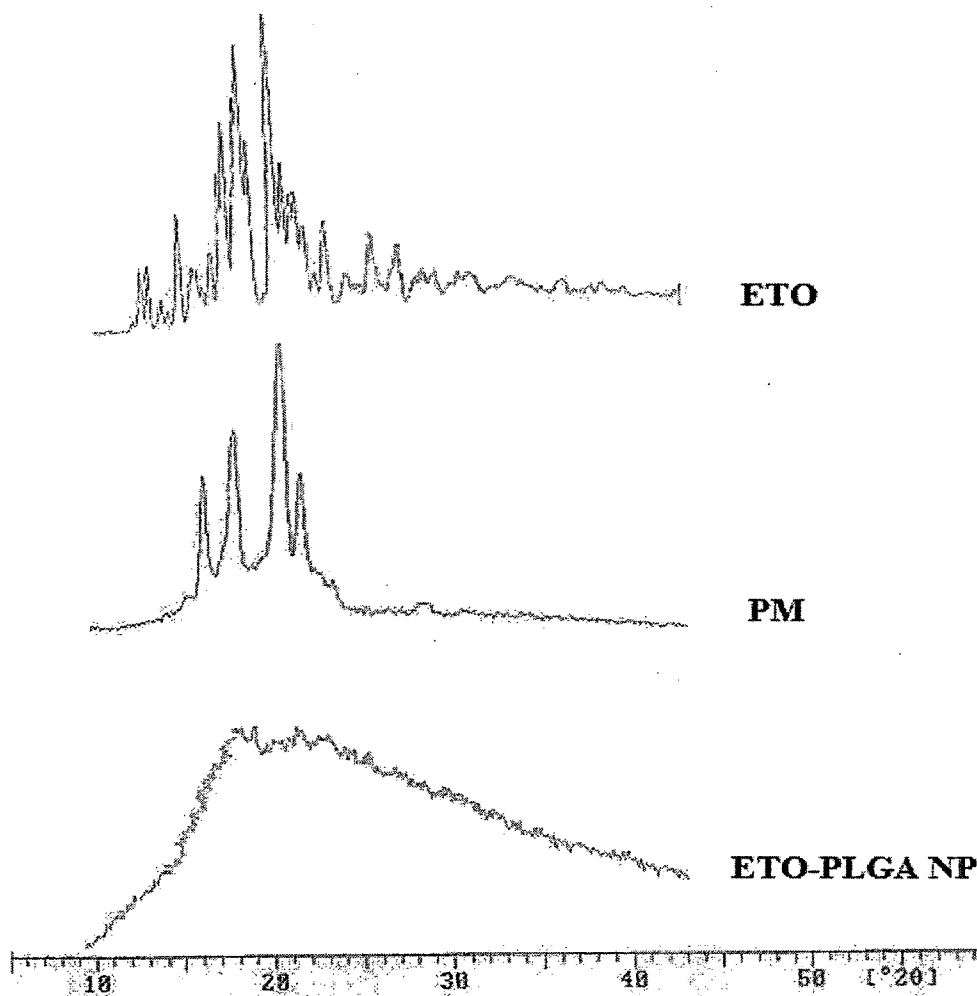


Fig. 4.11: XRD of Etoposide, PLGA and Etoposide loaded Nanoparticles

4.5.7 SEM studies

The electron micrographs showed spherical, discrete and homogenous particles in the nanometer size range (Fig. 4.12).

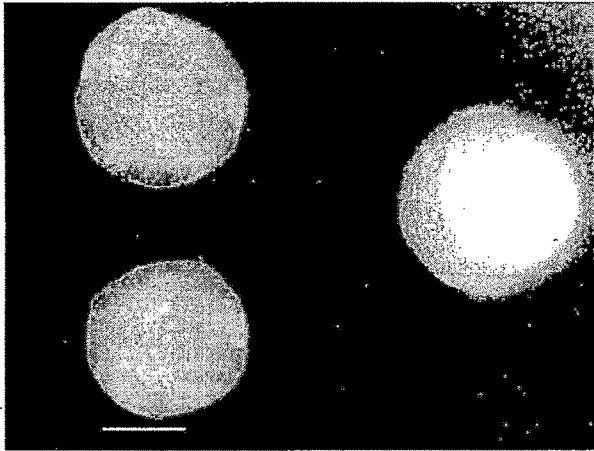


Fig. 4.12: SEM of Etoposide loaded PLGA NP (the bar in the figure indicates 50nm size)

4.5.8 Drug Release studies

In vitro drug release was carried out for the two optimized formulations ENP5 and ENP2. ENP5 had MPS of 112nm and EE of 77%. ENP2 on the other hand had higher EE of 83% but had a larger MPS of 160nm. The release study was carried out on lyophilized nanoparticles and was compared to the free drug. The drug release pattern is shown in Table 4.18 and Fig 4.13. 100% of the free drug was released in four hours, whereas, ENP5 nanoparticles showed a sustained release up to 36h and ENP2 showed sustained release up to 72h.

The initial release from both the NP was nearly the same, around 10% in 30 minutes. This initial release is said to be due to diffusion of dissolved drug initially deposited inside the pores of the particle (Cohen et al., 1991). The large surface to volume ratio of the NP geometry is also responsible for the initial fast release. The release pattern changed after the first hour for both the NPs. At the end of 24 h, nearly 80% of the drug was released from ENP5, where as only 55% of the drug was released from ENP2. At the end of 48 h nearly 99% of the drug was released from ENP5 but only 75% of the drug was released from ENP2. The difference in the release of the two NP was attributed to their different sizes, as otherwise they were similar in composition. ENP5 was of smaller size compared to ENP2 and the drug release pattern showed (Fig 4.12) that the drug from the smaller size NP released faster. Smaller nanoparticles lead to a shorter average diffusion path of the matrix entrapped and lead to faster release of the entrapped drug compared to bigger size NP (Mainardes et al., 2002). The larger nanoparticles of ENP2 could sustain the release of the drug up to 72h. The results obtained are in accordance with the study of some authors who claimed that the particle size differences is a significant factor for drug release rate kinetics in nanoparticulate drug delivery systems (Chorny et al. 2002; Park 1995).

The other factor responsible for the different release rate would be the amount of drug loading in each NP. ENP5 had higher drug loading (14%) than ENP2 (9%). It has been reported that an increase in the amount of drug in the nanoparticles not only increases the porosity of the system as the drug dissolves, but also, reduces the relative amount of polymeric material acting as a diffusional barrier (Radwan, 1995). Therefore NPs with a greater amount of drug content released more quickly.

Table 4.18
In Vitro Drug Release Profile of Etoposide and Etoposide loaded Nanoparticles

Time (h)	% Drug Released (\pm SD)		
	ETO	ENP5	ENP2
0.5	38.2 \pm 2.4	10.8 \pm 1.8	10.1 \pm 1.2
1	42.7 \pm 2.9	20.3 \pm 2.1	16.2 \pm 2.8
2	67.2 \pm 4.8	28.6 \pm 2.8	20.6 \pm 2.3
3	89.3 \pm 5.7	35.7 \pm 2.7	23.5 \pm 3.5
4	100.0 \pm 0.4	41.6 \pm 2.2	34.2 \pm 0.8
6		51.2 \pm 2.4	42.9 \pm 1.0
12		61.8 \pm 2.3	51.1 \pm 3.6
24		79.2 \pm 2.6	59.0 \pm 5.1
36		91.2 \pm 2.4	68.3 \pm 3.5
48		99.0 \pm 0.4	78.2 \pm 2.9
60			85.6 \pm 2.1
72			98.3 \pm 0.8

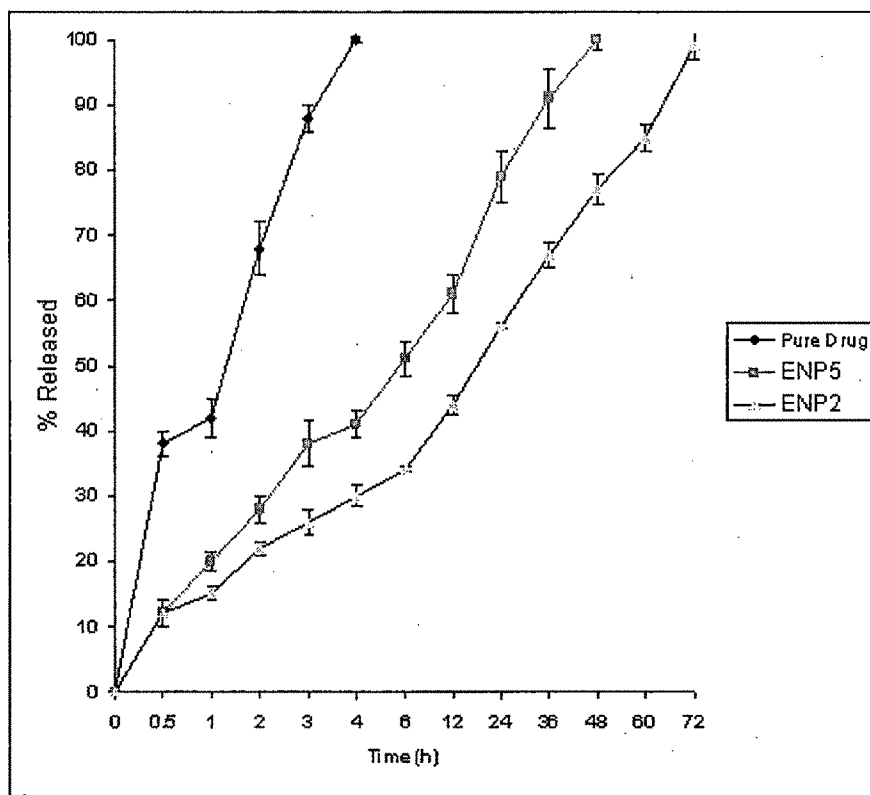


Fig. 4.13: In Vitro Drug Release Profile of Etoposide and Etoposide loaded Nanoparticles

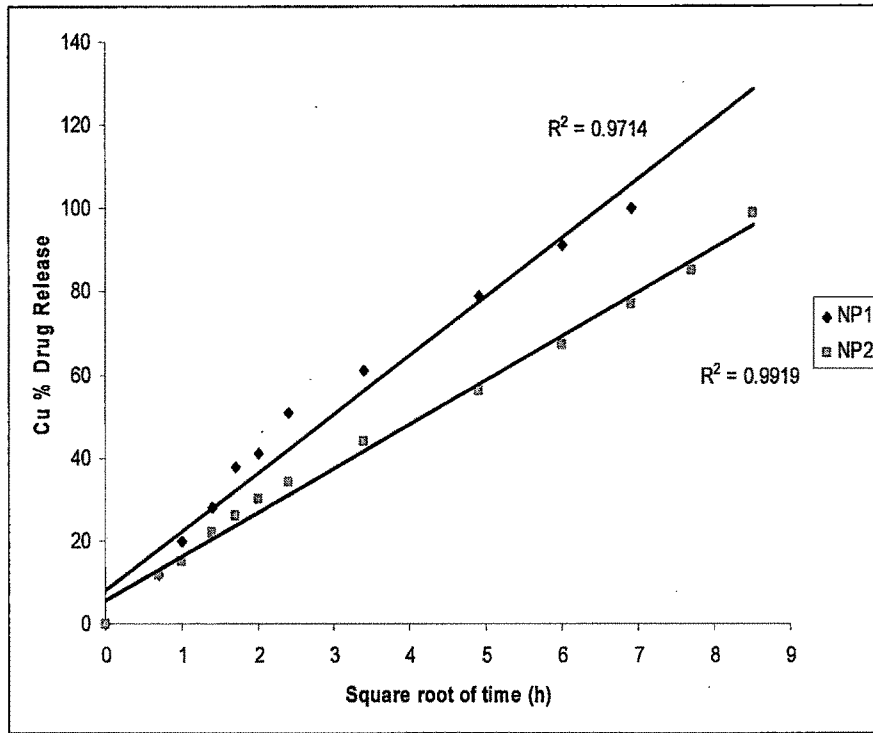


Fig 4.14: Drug Release Fitted to Higuchi Model

The data obtained from the drug release was fitted to different kinetic models to understand the drug release mechanism and kinetics. When the data was fitted to Higuchi model (Fig. 4.14) it was seen that ENP2 had a high correlation R^2 value > 0.99 but ENP5 had R^2 value of 0.9714. This indicated that the release from ENP2 followed Higuchi diffusion.

The release was fitted to both the zero order and first order models (Fig 4.13 and Fig 4.15). It was clearly evident from the linear graph of Fig 4.14a and 4.14b that the release followed first order release kinetics for both the nanoparticles as the R^2 value was more than 0.99 in both the cases. .

The drug release data was fitted to Korsmeyer-Peppas model (Fig. 4.16) to determine the value of diffusion exponent (n). The value of n for a spherical system is < 0.43 for Fickian release, $0.43 < n < 0.85$ indicates non-Fickian release, $n > 0.85$ indicates case II release (Siepmann and Peppas, 2001). The n values obtained from the slopes of the graphs from Fig. 4.16. The n value for both the nanoparticles was less than 0.43 therefore the release mechanism is said to follow Fickian diffusion kinetics.

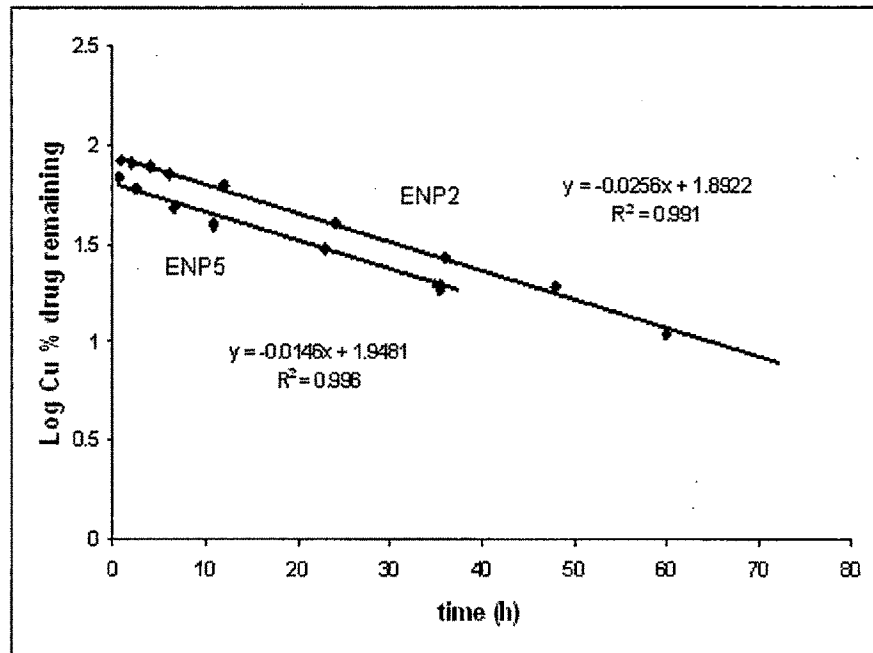


Fig 4.15: First order plot of Log cumulative % drug remaining Vs Time of ENP2 and ENP5

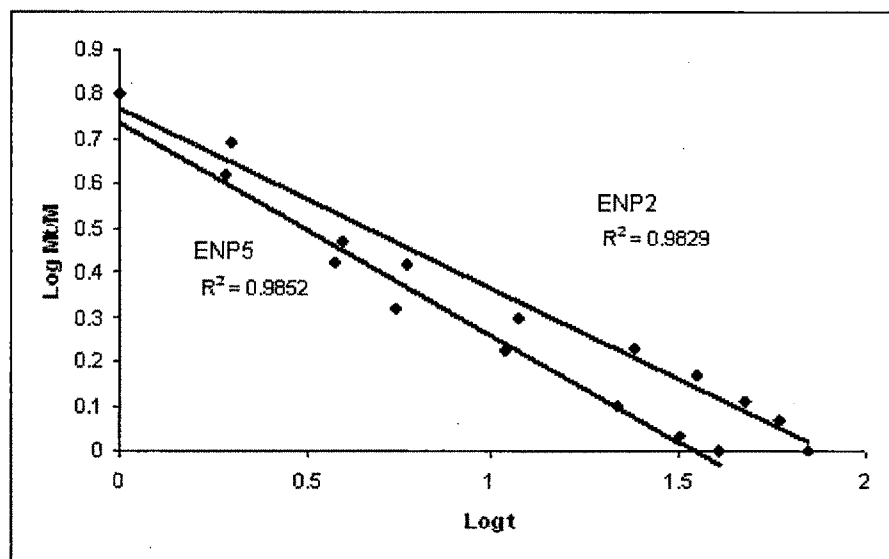


Fig 4.16: Korsmeyer-Peppas model for ENP2 and ENP5, $\text{Log } (M_t/M_\infty)$ is plotted against $\text{Log time } t$

Table 4.19
Summary of the R² values of zero, first, Higuchi, Korsmeyer-Peppas models and n value of Korsmeyer-Peppas model

Formulation	ENP5	ENP2
Zero order	0.9701	0.9760
R ² value		
First order	0.9910	0.9904
R ² value		
Higuchi	0.9714	0.9919
R ² value		
Korsmeyer-Peppas,	0.9852	0.9829
R ² value		
Korsmeyer-Peppas,	0.403	0.404
n value		

Table 4.19 gives a summary of the R² values of zero, first, Higuchi, Korsmeyer-Peppas models and n value of Korsmeyer-Peppas model. It can be concluded that the release of etoposide from the PLGA NP follows first order kinetics and mechanism of drug release is Fickian.

4.5.9 Stability studies

Stability studies of polymeric nanoparticles were carried out to evaluate the change in particle size and drug content of the drug over a period of 3 months (3M) at different storage conditions.

Effect of Storage at 2-8°C on MPS

For both the etoposide loaded PLGA NPs ENP5 and ENP2 there was no significant change ($P>0.05$) in the mean particle size at 2-8°C for 1, 2 and 3 M in the FD state (Fig 4.17) Similarly there was no significant change ($P>0.05$) in the mean particle size of ENP5 and ENP2 at 2-8°C for 1M for AD. But there was a significant change in the mean particle size of both ENP5 and ENP2 at 2-8°C for 2 and 3M for AD. The size of the particles increased significantly in the 3 months (Fig 4.16). The MPS of ENP5 (AD) increased from initial 112nm to 128 and 132 nm in 2 and 3M respectively The MPS of ENP2 (AD) increased from initial 168 nm to 175 and 178 nm in 2 and 3M respectively.

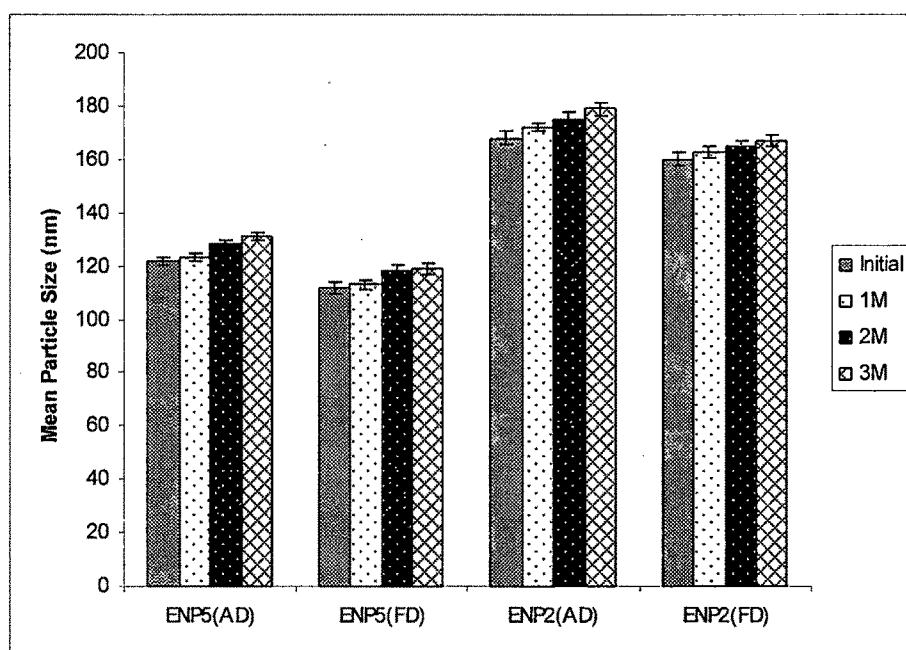


Fig. 4.17: Effect of storage condition at 2-8°C on Mean Particle Size of Etoposide loaded NP in Aqueous Dispersion and Freeze Dried. The values are mean of three batches with \pm S.D

Effect of storage at 25°C on MPS

For Etoposide loaded PLGA NPs ENP5 and ENP2 there was no significant change ($P>0.05$) in the mean particle size for 1M and 2M in FD state and no change in AD state till 1M (Fig 4.18). But there was a significant change in the mean particle size of both ENP5 and ENP2 at 25°C for 2 and 3M in AD state and 3M in FD state. The MPS of ENP5 (AD) increased from initial 122nm to 130 and 153 nm in 2 and 3M respectively. The MPS of ENP5 (FD) increased from initial 112 nm to 122 nm in the 3M. The MPS of ENP2 (AD) increased from initial 168 nm to 179 and 182 nm in 2 and 3M respectively. The MPS of ENP2 (FD) increased from initial 160nm to 169 nm in 3M.

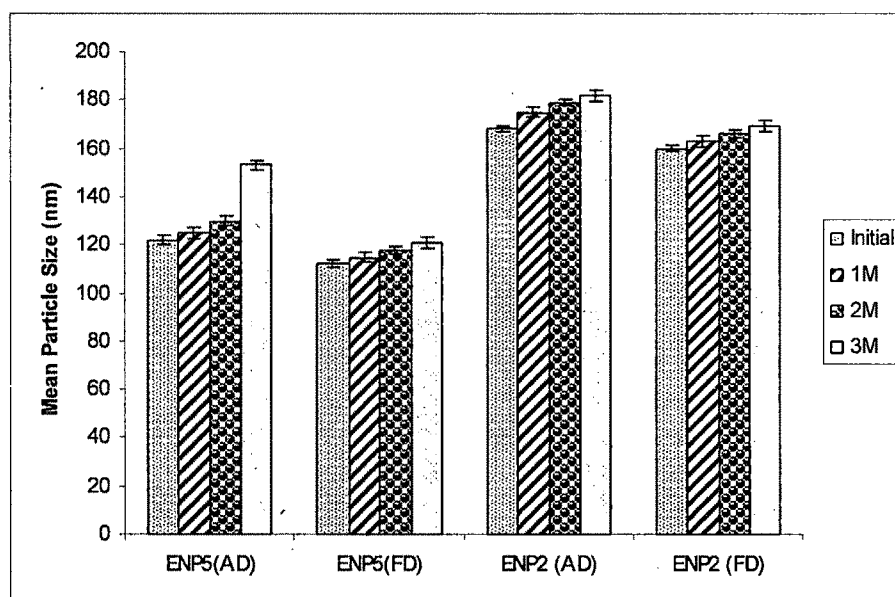


Fig. 4.18: Effect of storage condition at 25°C on Mean Particle Size of Etoposide loaded NP in Aqueous Dispersion and Freeze Dried. The values are mean of three batches with \pm S.D

Effect of storage at 40°C on MPS

Etoposide loaded PLGA NPs ENP5 and ENP2 were not stable at 40°C as there was significant change ($P>0.05$) the mean particle size (Fig. 4.19). The MPS of ENP5 (AD) increased from initial 122 nm to 132, 140 and 160nm in the 1, 2 and 3M respectively. The MPS of ENP5 (FD) increased from initial 112 nm to 127, 129 and 132nm in the 1, 2 and 3M respectively. The MPS of ENP2 (AD) increased from initial 168nm to 179, 185 and 197 nm in 1, 2 and 3M respectively. The MPS of ENP2 (FD) increased from initial 160nm to 169, 172 and 185 nm in 1, 2 and 3M respectively.

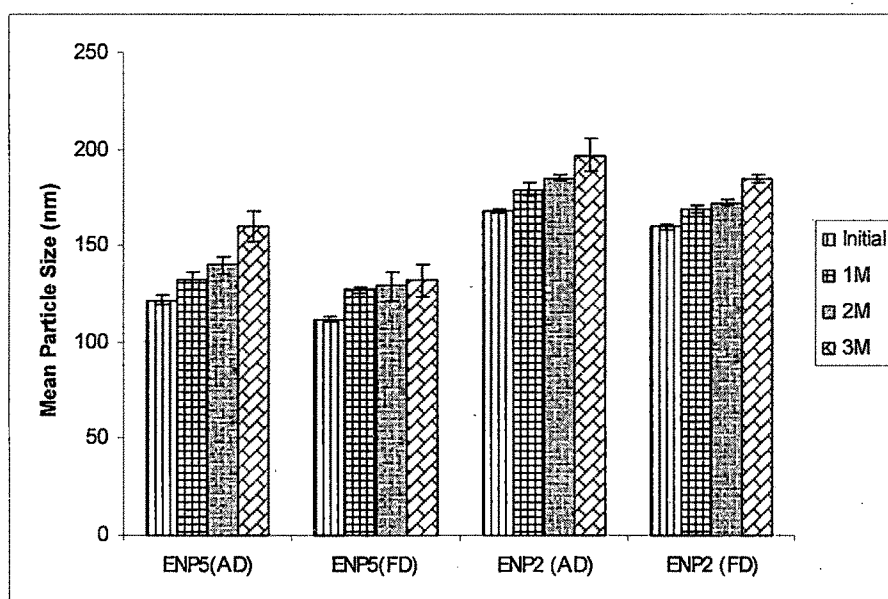


Fig. 4.19: Effect of storage condition at 40°C on Mean Particle Size of Etoposide loaded NP in Aqueous Dispersion and Freeze Dried. The values are mean of three batches with \pm S.D

Conclusion

It was concluded from the stability studies that Etoposide loaded PLGA NP were stable in terms of mean particle size at 2-8°C up to three months in the FD state, one month in the AD state at 2-8°C and for 1M in both the FD and AD state at 25°C. It has been reported that the mean particle size of nanoparticles increases over a period of time due to aggregation (Gasper MM et al., 1998). At higher temperature, the NPs were not stable as an increase in size was observed.

Effect of Storage at 2-8°C, 25°C and 40°C on Drug content of NP

There was no significant change ($P>0.05$) in the drug content for both ENP5 and ENP2 at 2-8°C upto 3 months FD state and for 1month in AD state as shown in the Fig 4.20a and Fig 4.20b.

At 25°C ENP5 showed no significant change in drug content for 1M in FD state but there was a significant change in 2 and 3M in the FD state. In the AD state the drug content kept on reducing with time and reduced to 80% in the third month. ENP2 was comparable more stable in FD state as it showed no significant change in drug content upto 2 months after which the drug content was reduced to 92% in the third month. In the AD state ENP2 was not stable and as time increased the drug content decreased from 93% in 1M to 85 and 78% in 2 and 3M respectively.

Both the formulations were unstable at 40°C and a significant change was observed in the drug content for both AD and FD state. The drug content in the third month was reduced to 84% and 75% for ENP5 in FD and AD state respectively. Similarly, drug content in the third month was reduced to 87% and 73% for ENP2 in FD and AD state respectively

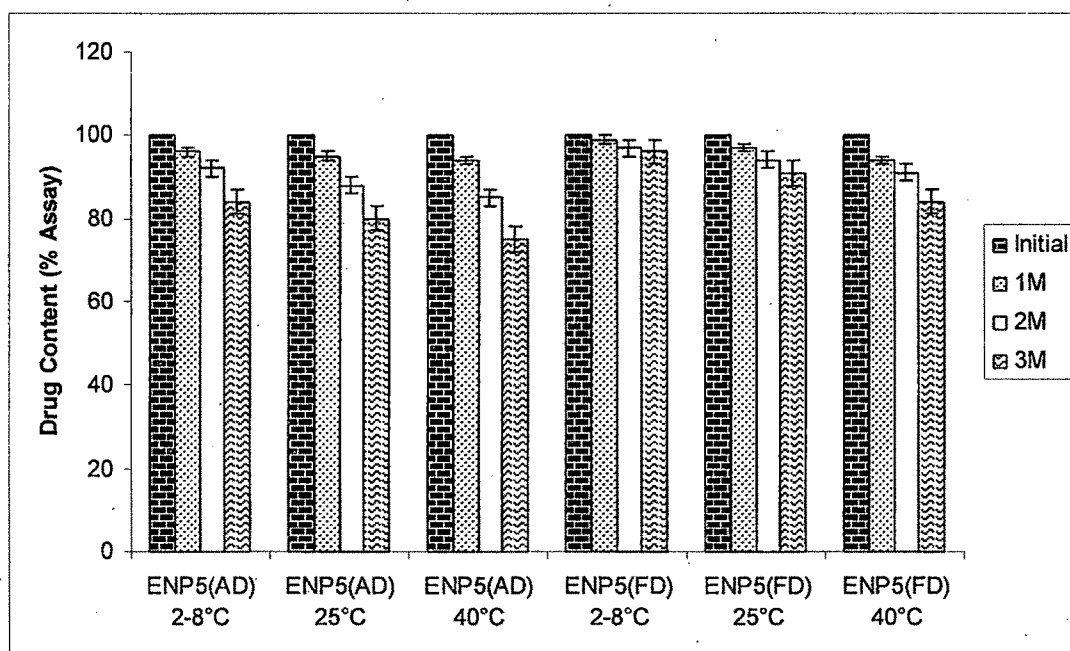


Fig. 4.20a: Effect of storage at 2-8°C, 25°C and 40°C on drug content of Etoposide loaded NP (ENP5) in FD and AD state. The values are mean of three batches with \pm S.D

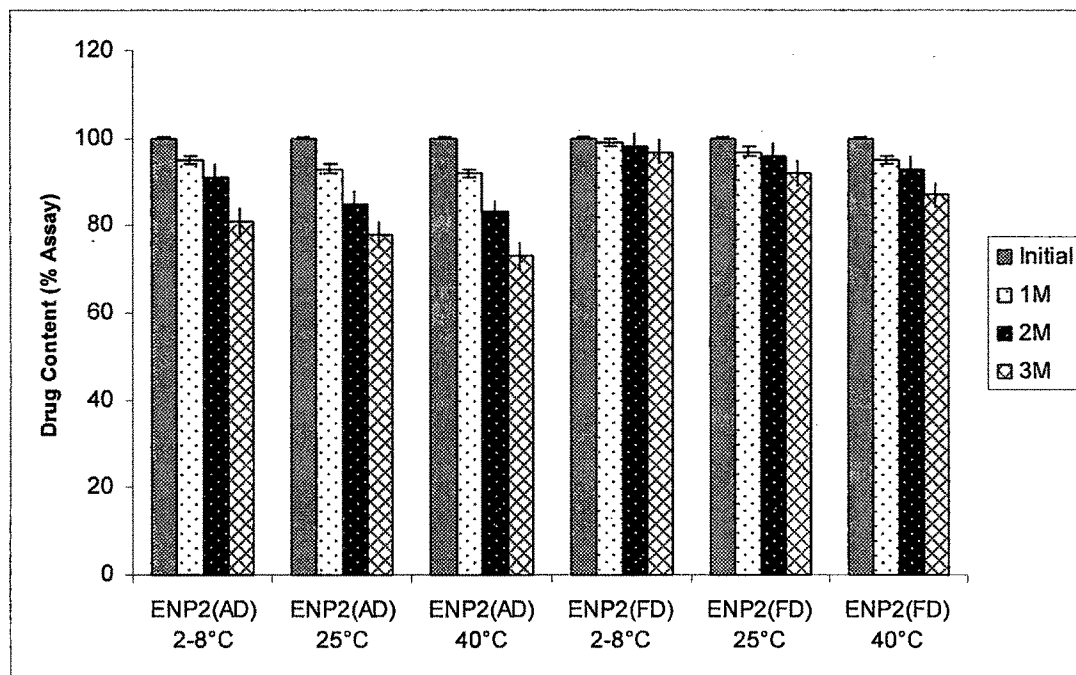


Fig. 4.20b: Effect of storage at 2-8°C, 25°C and 40°C on drug content of Etoposide loaded NP (ENP2) in FD and AD state. The values are mean of three batches with \pm S.D

Conclusion

It was observed that both the NP formulations were stable in terms of drug content up to 3 months in FD state and for 1 month in AD state at 2-8°C. ENP5 was stable up to one month in FD state at 25°C and ENP2 was stable up to two month in FD state at 25°C. The NP were not stable at 40°C, due to polymer degradation (Dunne et al., 2000).

It was concluded that it was best to store nanoparticle formulations in the freeze dried state at 2-8°C where they remained stable in terms of both MPS and drug content.

CHAPTER 4 B

FORMULATION DEVELOPMENT AND EVALUATION OF ETOPOSIDE LOADED PLGA-MPEG AND PLGA-PLURONIC NANOPARTICLES

4.6 Introduction

In order to be useful as controlled drug delivery the nanoparticulate drug carriers must show persistence in systemic circulation after intravenous administration. But these carriers, when given intravenously are rapidly cleared by the cells of the mononuclear phagocytes system (MPS). At present, many studies have concentrated on the development of stealth nanoparticles as drug carriers, which could avoid, or at least reduce the uptake by phagocytes and remain in circulation for an extended period of time.

Polyethyleneglycol (PEG) modified biodegradable polymer is one of the most popular materials to prepare stealth nanoparticles (Gref et al., 1994). Nanoparticles prepared from polyethyleneglycol-modified poly (D, L-lactide-co-glycolide) (PEG-PLGA) have been extensively investigated as drug carriers due to their controlled release, biodegradability and biocompatibility (Avgoustakis et al., 2003). After intravenous administration, the PLGA-PEG nanoparticles remain in the systemic circulation for hours, whereas the PLGA nanoparticles are removed from blood within few minutes. The PEG layer provides a steric barrier to the particle and its opsonization is reduced. As a result these particles have been shown to long circulating. Long-circulating nanoparticles made of methoxypoly(ethylene glycol)- poly(lactide-co-glycolide) (mPEG-PLGA) also have a good safety profiles and provide drug-sustained release.

Pluronic is a triblock copolymer composed of polyethyleneoxide and propyleneoxide (PEO-PPO-PEO) (Alexandridis, 1995). Illum et al. (1984) have shown that Pluronic coated PLGA nanoparticles avoided recognition by MPS and were long circulating.

In the present study we synthesised PLGA-mPEG and PLGA-PLURONIC copolymers and prepared their drug loaded NPs.

4.7 Synthesis of PLGA-mPEG copolymer

Poly(lactide-co-glycolide)-monomethoxy(polyethyleneglycol) copolymer (PLGA-mPEG) was synthesized by the ring opening polymerization by melting PLGA and mPEG and using stannous octoate as catalyst (Beletsi et al., 1999). PLGA and MPEG were mixed in a 5:1 molar ratio and added in a 10ml flask at 140°C in presence of nitrogen. 0.05% w/w of stannous octoate was added and reacted at 180°C for 3 hours. The resultant product was dissolved in methylene chloride and then precipitated in excess cold diethyl ether. The precipitate was filtered, and dried under reduced pressure to obtain PLGA-mPEG. The copolymer was analyzed by ¹H-NMR and FTIR.

4.8 Synthesis of PLGA-PLURONIC copolymer

PLGA and Pluronic F-68 were blended together in a 2:1 w/w ratio and dissolved in minimum amount of chloroform in a flask (Tobio et al., 1999). The solvent was removed under vacuum overnight and the resultant copolymer was analyzed by FTIR.

4.9 ¹H-NMR and Fourier Transform - Infrared Spectrum

¹H-Nuclear Magnetic Resonance (¹H-NMR) was used to study the MPEG content of the copolymer PLGA-mPEG. The copolymer was dissolved in CDCl₃ and then NMR spectrometer (Varian VXR 300, USA) was used to study composition of the copolymer.

The Fourier transform infrared spectrum (FT-IR) was recorded for PLGA, mPEG, PLGA-mPEG copolymer, Pluronic F-68 and PLGA-PLURONIC copolymer. The polymer was casted into a neat film by first dissolving in chloroform and then evaporating the solvent. The dried film was then kept between KBr disc and the spectrum was recorded using Perkin Elmer 1700 spectrometer (USA).

4.10 Preparation of Etoposide loaded PLGA-mPEG nanoparticles and PLGA-Pluronic nanoparticles

Nanoparticles were prepared by oil-in-water single-emulsion solvent evaporation using high pressure homogenization by using the copolymer (PLGA-mPEG or PLGA-Pluronic) as described in preparation of etoposide loaded PLGA nanoparticles (section 4.2). The method was optimized for different parameters like- drug:polymer ratio and surfactant concentration on the basis of size and entrapment efficiency.

4.11 Evaluation of Nanoparticles

The prepared NP were evaluated for Mean Particle Size and Polydispersity index, Entrapment Efficiency, Surface charge, XRD Studies and Scanning Electron Microscopy. In vitro drug release and mathematical modeling of drug release kinetics were studied for optimized batches. The methods used are the same described in section 4.3 .

4.12 Stability study of Nanoparticles

The freeze dried samples and aqueous dispersion (without freeze drying) were sealed in Type-I amber colored glass vials. The samples were stored at 2-8°C, 30°C and 40°C. Samples were withdrawn at 1, 2 and 3 months time interval and analyzed for mean particle size and assay. The study was performed in triplicate.

4.13 Results and Discussions

4.13.1 ^1H -NMR Spectrum

^1H NMR spectra of PLGA-mPEG is shown in Fig. 4.21. The copolymer shows peaks at 5.3 and 4.8 ppm, corresponding to the lactic acid proton ($-\text{O}-\text{CH}^*(\text{CH}_3)-\text{CO}-$) and the glycolic acid protons ($-\text{O}-\text{CH}_2^*-\text{CO}-$), respectively. The peak at 1.8 ppm was attributed to the $-\text{CH}_3^*$ of the lactic repeat units of the copolymer. The peak at 3.6 ppm of methene protons ($-\text{CH}_2-$) is due to the PEG segment (Jeong et al., 1999). Thus, the results of the ^1H NMR study confirms the formation of PLGA-mPEG copolymer.

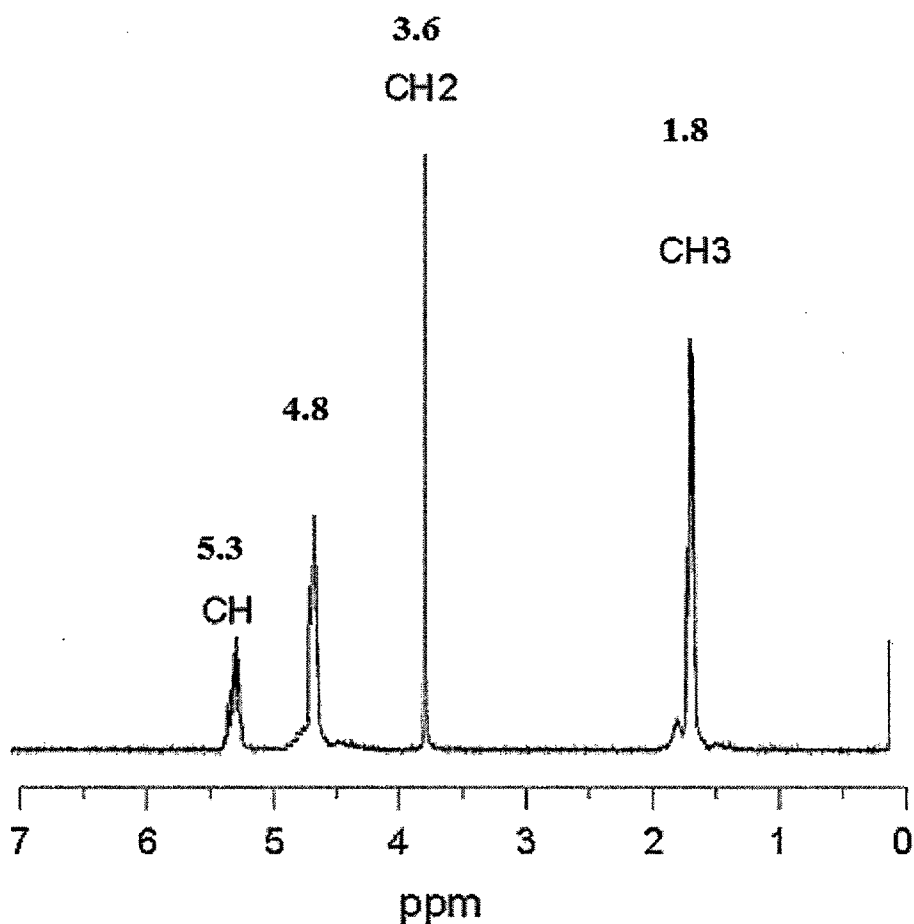


Fig 4.21: ^1H NMR spectra of PLGA-mPEG copolymer

4.13.2 FT-IR Spectrum

The FT-IR spectrum of PLGA, mPEG and PLGA-mPEG is shown in Fig. 4.22. In the PLGA spectrum, the broad peak at 3500 cm^{-1} indicated $-\text{OH}$ stretching, peak at 2900 cm^{-1} indicated C-H stretch and peak at 1100 cm^{-1} was attributed to C-O stretch. The spectrum of mPEG showed peaks at 3500 cm^{-1} , 2900 cm^{-1} and 1200 cm^{-1} indicating $-\text{OH}$ stretch, C-H stretch and C-O stretch respectively. In the PLGA-mPEG spectrum, the peaks at 2900 cm^{-1} indicated C-H stretch, strong absorption peak at 1760 cm^{-1} belonged to $-\text{C}=\text{O}$ stretch and peak at 1100 cm^{-1} was attributed to C-O stretch. The broad peak at 3500 cm^{-1} , indicating $-\text{OH}$ stretching, was practically eliminated from the spectrum of mPEG-PLGA, indicating the formation of the copolymer (Yang et al., 2006). Comparison of FT-IR spectrum of three polymers confirmed the formation of the copolymer PLGA-mPEG.

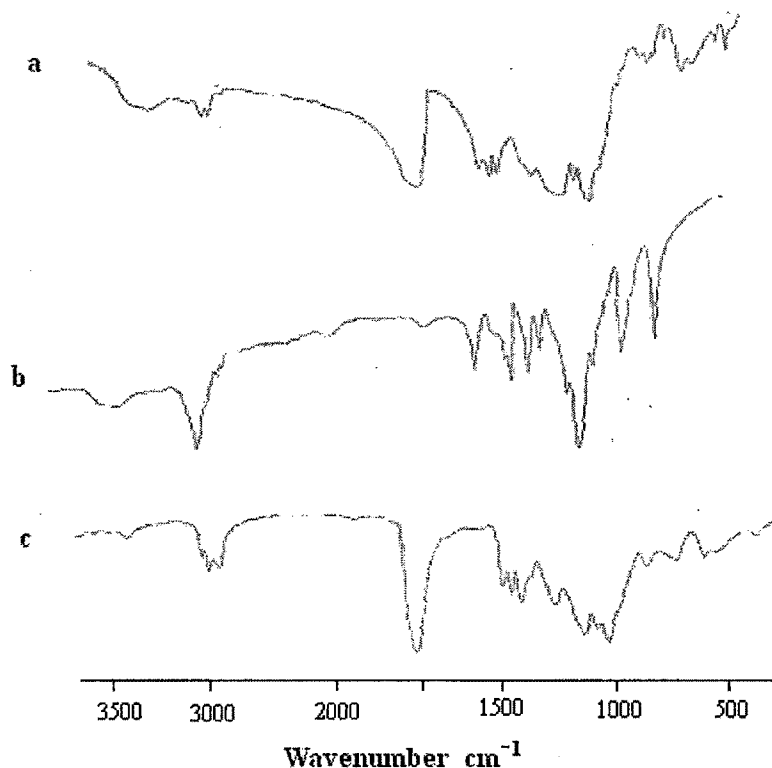


Fig. 4.22: FT-IR spectra of (a) PLGA, (b) mPEG and (c) PLGA-mPEG

Fig. 4.23 shows FT-IR spectra of (a) PLGA, (b) Pluronic F-68 and (c) PLGA-PLURONIC. As shown in the Fig. 4.23a, the broad peak at 3500 cm^{-1} indicated $-\text{OH}$

stretching, absorption peak at 2900 cm^{-1} was corresponding to the C-H stretch and peak at 1100 cm^{-1} was attributed to C-O stretch. Pluronic (Fig. 4.23b) showed characteristic bands at 2880 cm^{-1} and 1120 cm^{-1} , which correspond to alkyl and ether groups, respectively. In the PLGA-PLURONIC spectra (Fig. 4.23c) ether groups of Pluronic showed a displacement to the lower wavelength (from 1120 cm^{-1} to 1100 cm^{-1}). The broad peak at 3500 cm^{-1} (corresponding to OH stretching) visible in both PLGA and Pluronic was practically eliminated from the spectrum of PLGA-PLURONIC. Comparison of FT-IR spectrum of three polymers confirmed the formation of PLGA-PLURONIC copolymer.

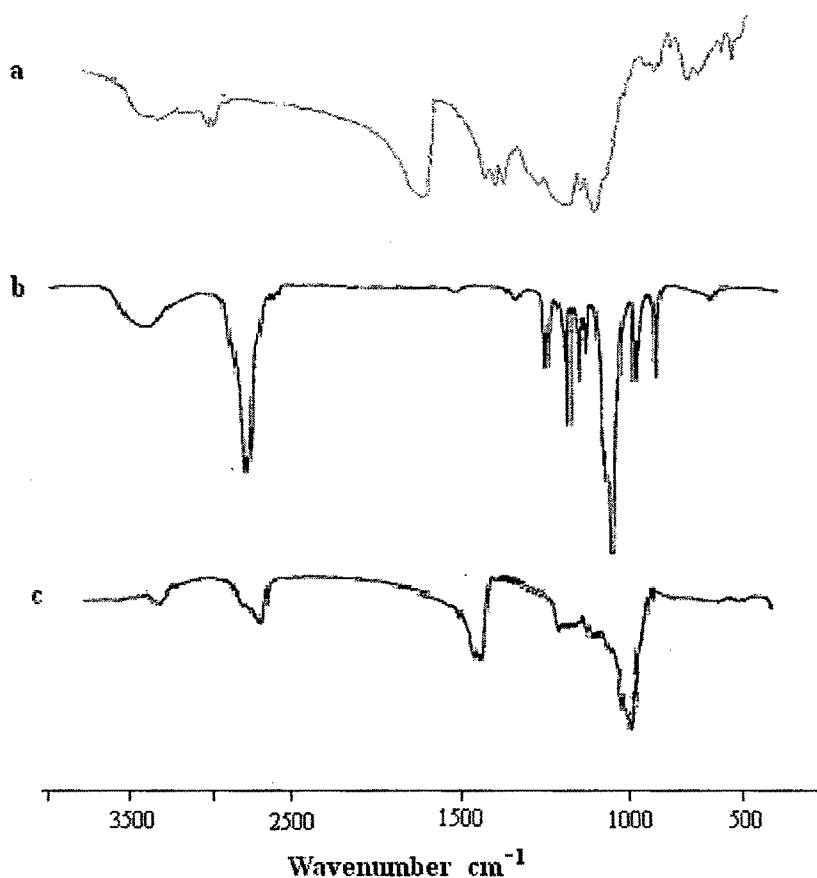


Fig. 4.23: FT-IR spectra of (a) PLGA, (b) Pluronic F-68 and (c) PLGA-PLURONIC

4.13.3 Optimization of Etoposide Loaded PLGA-MPEG NP Using Factorial Design

4.13.3.1 Response -Mean particle size (MPS)

Nine formulations were prepared as per 3^2 Factorial Design. The real values and the transformed values of different batches for PLGA-MPEG NP for the response of Mean particle size (MPS) are shown in Table 4.21. The results of the regression output and ANOVA are presented in Table 4.22 and Table 4.23 respectively. The mean particle size of NP ranged from 94.02 ± 3.4 nm to 132.9 ± 11.3 nm. The response in the equation Y1 is the quantitative effect of the formulation components or independent variables X1 and X2. The equations for the full model is given below-

Full Model for PLGA-MPEG NP

$$Y_1 (\text{MPS}) = 104.33 + 1.1666X_1 - 8.333X_2 + 18.5X_1^2 - 2X_2^2 - 1.5X_1X_2 \quad (4.8)$$

The positive sign for the co-efficient of X1 in equation 1 show that MPS can be increased by an increase in X1. However the negative sign for the coefficients of X2 in equation 1 show that mean particle size can be decreased by an increase in X2.

The polynomial model (equation1) was found to be significant with an F value of 405.48 ($p=0.000193$). The value of correlation coefficient was found to be 0.9985, indicating a good fit. The data from equation 1 reveals that both the factors (X_1 and X_2) affect the parameter Y_1 . The low value of X_1X_2 coefficient also suggests that the interaction between X_1 and X_2 is not significant.

Table 4.20
Formulation of Etoposide loaded PLGA-MPEG NP by 3² factorial design:
Factors, their levels and transformed Values, Response: MPS

Batch No.	Real value		Transformed values					Response
	Drug: Polymer ratio (mg) X1	Surfactant Conc. (% w/v) X2	X1	X2	X1 ²	X2 ²	X1X2	MPS (nm) ± SD*
1	1:10	0.5	-1	-1	1	1	1	127.3 ±11.4
2	1:10	1.0	-1	0	1	0	0	121.3 ±13.4
3	1:10	1.5	-1	1	1	1	-1	113.8 ±9.4
4	1:6	0.5	0	-1	0	1	0	110.5 ±5.2
5	1:6	1.0	0	0	0	0	0	105.9 ±5.8
6	1:6	1.5	0	1	0	1	0	94.02 ±3.4
7	1:4	0.5	1	-1	1	1	-1	132.9 ±11.3
8	1:4	1.0	1	0	1	0	0	124.4 ±3.8
9	1:4	1.5	1	1	1	1	1	112.6 ±7.6

* All the tests were carried out in triplicate

Table 4.21
Model coefficients estimated by multiple linear regression for Response-MPS

Factor	Coefficient	Coefficient calculated value	Computed t- value	P-value
Intercept	β_0	104.3333333	187.8	3.33E-07
X1	β_1	1.166666667	3.834058	0.031275
X2	β_2	-8.333333333	-27.3861	0.000107
X1 ²	β_{11}	18.5	35.10128	5.08E-05
X2 ²	β_{22}	-2	-3.79473	0.032119
X1X2	β_{12}	-1.5	-4.02492	0.027556

Table 4.22
Analysis of Variance (ANOVA) of full model for Response-MPS

	DF	SS	MS	F	Significance F	R ²	Adj R ²
Regression	5	1126.333	225.266	405.48	0.000193	0.9985	0.9960
Error	3	1.666667	0.555556				

The predicted and observed values of response parameters are shown in Table 4.23. Low residual values showed that there was a reasonable agreement of predicted values and experimental values and % error below 5% showed the significance of the model used.

Table 4.23
Observed responses and Predicted values for Response-MPS

Batch No.	Observed value	Predicted value	Residual value	% Error
1	127.3	126.5	0.5	0.392
2	121.3	121.6666667	-0.666	0.494
3	113.8	112.8333333	0.166	0.145
4	110.5	110.6666667	-0.666	0.605
5	105.9	104.3333333	0.666	0.623
6	94.02	94	0	0.000
7	132.9	131.8333333	0.166	0.125
8	124.4	124	0	0.000
9	112.6	112.1666667	-0.166	0.147

The combined effect of factors X_1 and X_2 can further be elucidated with the help of response surface and contour plots (Fig. 4.24a and 4.24b respectively) which demonstrates that there is a linear fall in particle size from 115nm to 95 nm when the surfactant concentration (X_2) is between 1.0 to 0.0 and drug: polymer concentration (X_1) is between -1.0 to 0.0. However there is a linear rise in particle size from 111 nm to 130 nm when the surfactant concentration changes from 0.0 to -1.0 and drug: polymer concentration is between 0.0 and 1.0. From this discussion, one can conclude that appropriate selection of the levels of X_1 and X_2 yields optimum values of MPS.

Chapter 4 - Etoposide Loaded PLGA based Nanoparticles
 Section B- PLGA mPEG and PLGA-Pluronic NP

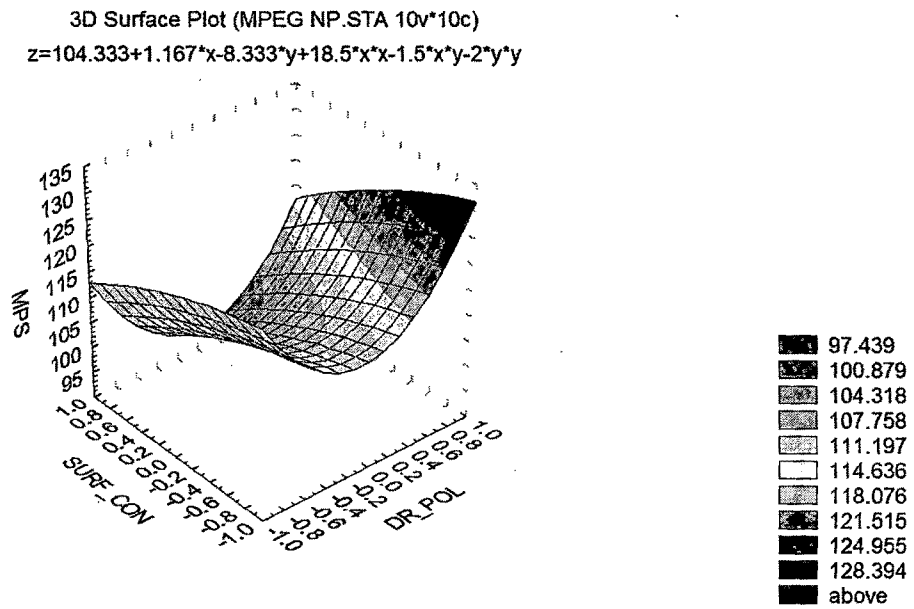


Fig 4.24a: Surface plot for MPS PLGA-MPEG NP

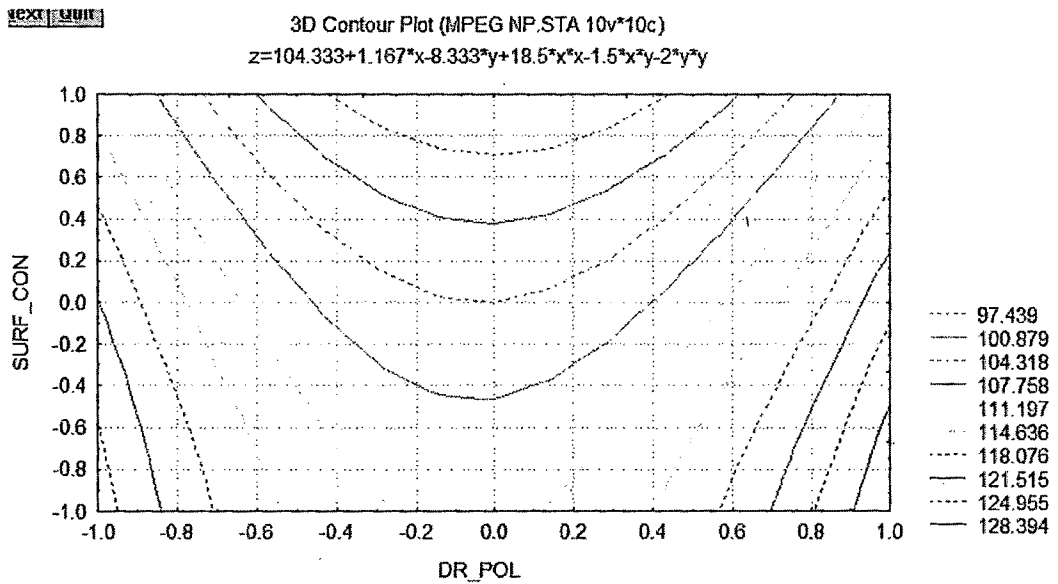


Fig 4.24b: Contour plot for MPS PLGA-MPEG NP

4.13.3.2 Response - %EE PLGA-MPEG NP

The different batches of PLGA-MPEG NP using 3^2 factorial design, their levels and transformed values for the response of %EE are shown in Table 4.24. The results of the regression output and ANOVA for both the full model and reduced model of PLGA-MPEG NP are presented (Table 4.25 and Table 4.26). The %EE of Eto varied from $62.09 \pm 3.13\%$ to $71.22 \pm 1.1\%$. The highest %EE was observed at medium level (0) of X1 (1:6) and highest level of X2 (1.5%w/v) (Batch B6). The regression equations for the models (full and reduced), Y1 and Y2 are as follows-

Full Model for PLGA-MPEG NP

$$Y2 (\%EE) = 70.57 + 1.208X1 - 0.24X2 - 6.091X1^2 - 0.121X2^2 + 0.432X1X2 \quad (4.9)$$

Reduced Model for PLGA-MPEG NP

$$Y2 (\%EE) = 70.57 + 1.208X1 - 6.091X1^2 + 0.432X1X2 \quad (4.10)$$

Based on the equation of the full model for equation 2, the positive sign for the coefficient of X1 shows that %EE can be increased by an increase in X1. However the negative sign for the coefficients of X2 in the equation 2 shows that %EE can be decreased by an increase in X2.

The results show that % EE greatly depend on the concentration of the surfactant used, an increase in the surfactant concentration from 0.5 to 1.5% markedly decreased the % EE. Based on the results of the multiple regression analysis and F statistics, it was concluded that the highest %EE could be obtained when X1 was kept at medium level (0) and X2 at the highest level (1).

Table 4.24

**Formulation of Etoposide loaded PLGA MPEG NP batches for 3²factorial design:
Factors, their levels and transformed Values, Response: %EE**

Batch No.	Real value		Transformed values					Response
	Drug: Polymer ratio (mg)	Surfactant Conc. (% w/v)	X1	X2	X1 ²	X2 ²	X1X2	% EE ± SD*
1	1:10	0.5	-1	-1	1	1	1	64.21±2.39
2	1:10	1.0	-1	0	1	0	0	63.27±3.42
3	1:10	1.5	-1	1	1	1	-1	62.09±3.13
4	1:6	0.5	0	-1	0	1	0	70.20±1.4
5	1:6	1.0	0	0	0	0	0	70.05±0.2
6	1:6	1.5	0	1	0	1	0	71.22±1.1
7	1:4	0.5	1	-1	1	1	-1	65.50±1.49
8	1:4	1.0	1	0	1	0	0	66.21±2.4
9	1:4	1.5	1	1	1	1	1	65.11±3.2

* All the tests were carried out in triplicate

To identify the effect of significant variables, the reduced model was generated by eliminating the X2 and X2² coefficients as their p value was more than 0.5. The R² value for the full model was 0.97067, where as for the reduced model the R² value was 0.966063. the reduced model is a significant one is shown by an increase in the adjusted R² value. Adjusted R² value was 0.92179 for the full model where as it increased to 0.9457 for the reduced model, hence the reduced model was sought.

Table 4.25
Model coefficients estimated by multiple linear regression for Response: % EE

Factor	Coefficient	Coefficient calculated value		P-value	
		Full Model	Reduced Model	Full Model	Reduced Model
Intercept	β_0	70.57111111	70.49	2.03E-06	1.86E-10
X1	β_1	1.20833333	1.208333	0.048746	0.011891
X2	β_2	-0.2483333		0.555914	
X1 ²	β_{11}	-6.0916667	-6.09167	0.002583	9.77E-05
X2 ²	β_{22}	-0.1216667		0.863639	
X1X2	β_{12}	0.4325	0.4325	0.416664	0.310593

Table 4.26a
Analysis of Variance (ANOVA) of Full model for Response: % EE

	DF	SS	MS	F	Significance F	R ²	Adj R ²
Regression	5	84.12506944	16.82501	19.8594	0.016604	0.97067	0.92179
Error	3	2.541619444	0.847206				

Table 4.26b
Analysis of Variance (ANOVA) of Reduced model for Response: % EE

	DF	SS	MS	F	Significance F	R ²	Adj R ²
Regression	3	83.72545	27.90848	47.44337	0.000427	0.966063	0.9457
Error	5	2.941242	0.588248				

The predicted and observed values of response parameters are shown in Table 4.27. Low values of the relative error showed that there was a reasonable agreement of predicted values and experimental values.

Table 4.27
Observed responses and Predicted values for Response: % EE

Batch No.	Observed value	Predicted value		Residual value		% Error	
		Full Model	Reduced Model	Full Model	Reduced Model	Full Model	Reduced Model
1	64.21	63.830	63.622	0.379	0.587	0.590	0.914
2	63.27	63.271	63.19	-0.001	0.08	0.001	0.126
3	62.09	62.468	62.757	-0.378	-0.667	0.608	1.074
4	70.2	70.697	70.49	-0.497	-0.29	0.698	0.413
5	70.05	70.571	70.49	-0.521	-0.44	0.739	0.628
6	71.22	70.201	70.49	1.018	0.73	1.422	1.025
7	65.5	65.381	65.174	0.118	0.325	0.180	0.496
8	66.21	65.687	65.606	0.522	0.603	0.788	0.910
9	65.11	65.750	66.039	-0.640	-0.929	0.983	1.427

Three dimensional surface response plots and two dimension contour plots are shown in Fig. 4.25a and 4.25b for the response of %EE of PLGA-MPEG NP. The plots were found to be non-linear with upward and downward segments which indicate non-linear relationship between X1 and X2 variables. There is a rise in % EE as the drug: polymer ratio is increased from -1.0 to 0.0 and as there is a further increase in drug: polymer ratio from 0.0 to 1.0 there is a decrease in % EE from 73% to 63%. The plots clearly indicate

Chapter 4 - Etoposide Loaded PLGA based Nanoparticles
 Section B- PLGA mPEG and PLGA-Pluronic NP

that there was no effect of surfactant concentration on EE. An EE of 70% could be obtained by keeping the values of X1 (Drug: polymer ratio) between -0.3 to 0.4.

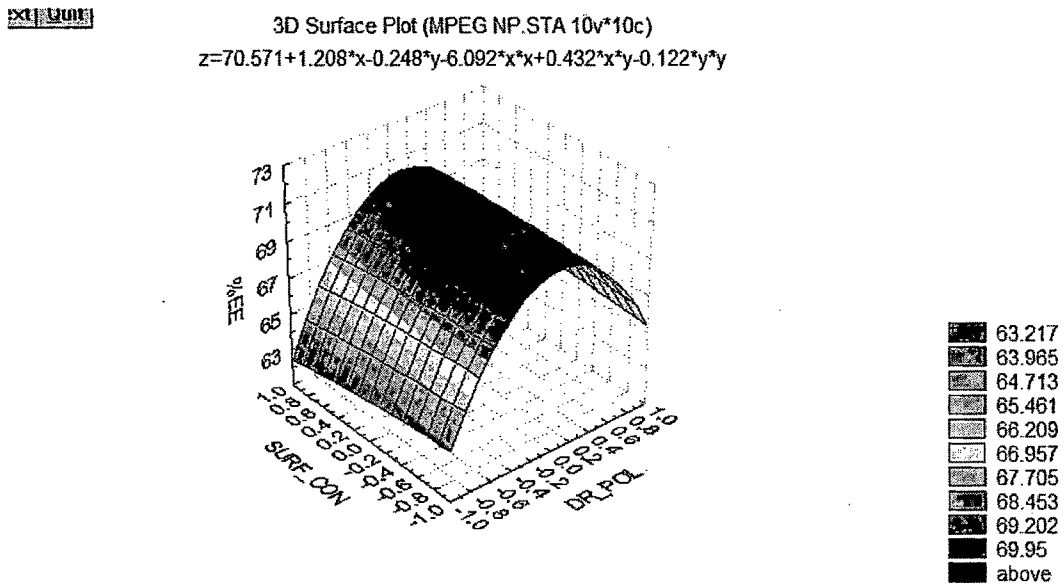


Fig 4.25a: Surface plot %EE MPEG NP

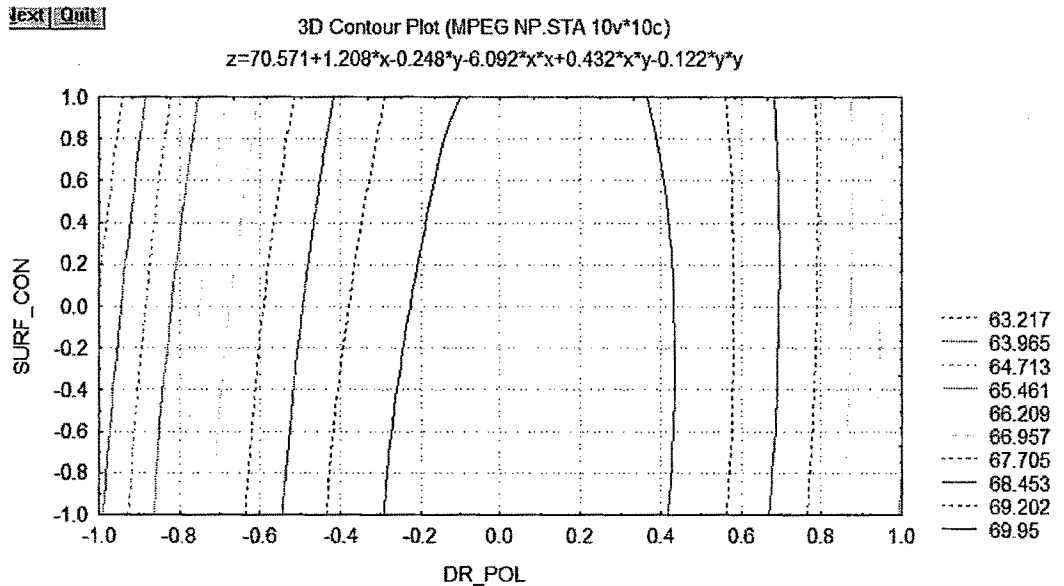


Fig 4.25b: Contour plot %EE MPEG NP

4.13.4 Zeta potential of PLGA-mPEG NP

The zeta potential (in PBS, pH 7.4) values of the different batches are shown in Table 4.28. The zeta potential values ranged between -6.0 mV to -8.9 mV for PLGA-mPEG NP. The optimized batch (based on least MPS and highest EE) had zeta potential value of -6.9 ± 1.3 mV (EPMPEG NP6). Figure 4.26 shows Zeta potential distribution of PLGA-mPEG NP, showing one sharp peak (-8.0 mV) signifying homogeneous distribution of surface charge on the particles. Table 4.28 and Fig. 4.27 shows the effect of surfactant concentration on Zeta potential of PLGA-mPEG NP and it was observed that zeta potential decreased with increase in the concentration of surfactant.

	Mean (mV)	Area (%)	Width (mV)
Zeta Potential (mV): -6.9	Peak 1: -8.0	100.0	1.4
Zeta Deviation (mV): 1.4	Peak 2: 0.00	0.0	0.00
Conductivity (mS/cm): 0.038	Peak 3: 0.00	0.0	0.00

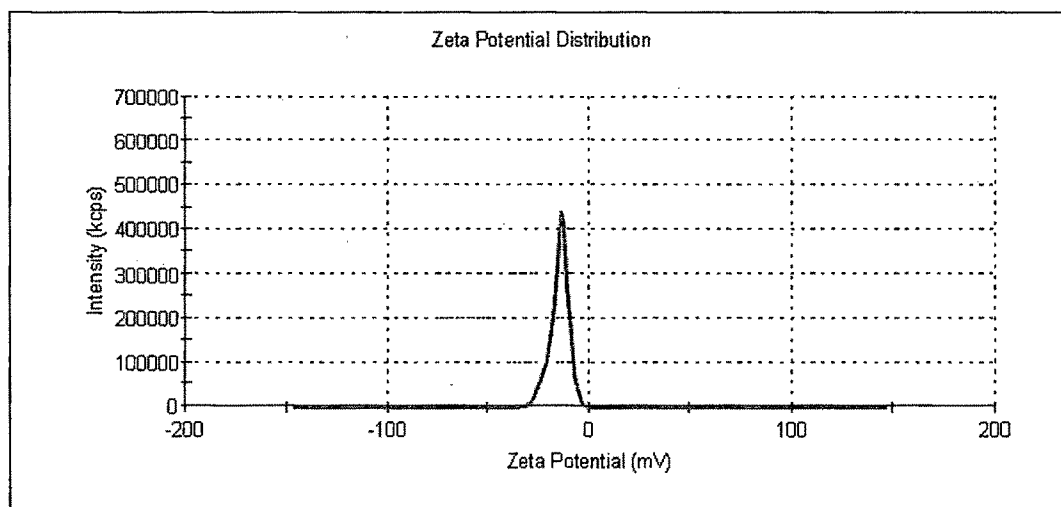


Fig. 4.26: Zeta potential of PLGA-mPEG NP (Batch No. EPMPEG NP6)

Table 4.28
Zeta Potential values of different batches of Etoposide loaded PLGA-mPEG NP

Batch No.	EPMPEG NP1	EPMPEG NP2	EPMPEG NP3	EPMPEG NP4	EPMPEG NP5	EPMPEG NP6	EPMPEG NP7	EPMPEG NP8	EPMPEG NP9
Drug:	1:10	1:10	1:10	1:6	1:6	1:6	1:4	1:4	1:4
Poly Ratio									
Surf Conc.	0.5	1.0	1.5	0.5	1.0	1.5	0.5	1.0	1.5
Zeta Poten (mV)	-8.9 ±1.4	-7.6 ±1.2	-6.0 ±0.8	-8.2 ±1.1	-7.3 ±2.1	-6.9 ±1.3	-7.7 ±0.7	-7.0 ±0.9	-6.5 ±1.6

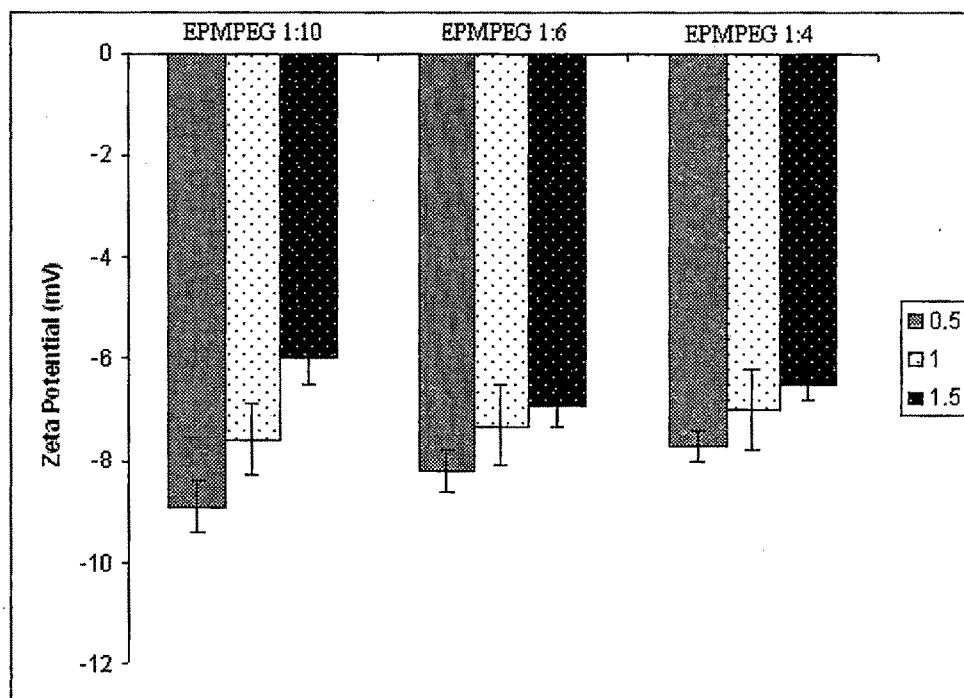


Fig. 4.27: Effect of surfactant concentration on Zeta potential of PLGA-mPEG NP

It is generally expected that greater the zeta potential of the nanoparticle, it is more likely to be stable because the charged particles repel each other. However, this rule cannot be strictly applied to systems containing steric stabilizers, because adsorption of the steric stabilizers would decrease the zeta potential due to shift in the shear plane of the particle (Heurtault et al., 2003). Weiss et al. (2006) prepared Fluorescence labeled PLGA nanoparticles and reported a stable NP having a less negative surface charge of -1.4 mV which was attributed to the presence of PVA on the surface. The steric stabilizer polymers may reduce the surface charge but still keeps the NP stable by creating a shield between the NP surface and the surrounding medium thereby protecting the nanoparticles from aggregation (Konan et al., 2003). Avgoustakis et al (2003) reported low negative zeta potentials of -4.3 to -6.4 mV for PLGA-mPEG NPs which were sterically stable.

Hence it was concluded that the PLGA-mPEG NP would be stable due to presence of mPEG on the surface, which would create a shield between the NP surface and the surrounding medium thus masking the charged groups on the surface and preventing the particles from aggregation.

4.13.5 Optimization of Etoposide Loaded PLGA-PLURONIC NP

The Eto loaded PLGA-Pluronic NP were prepared by high pressure homogenization using solvent evaporation method and were characterized for particle size, zeta potential and entrapment efficiency. The NPs formed were uniform, discrete and less than 200 nanometers in size. Nine batches were prepared by varying drug: polymer ratio and concentration of the surfactant (Table 4.29). The values obtained for mean particle size, zeta potential and percent of drug entrapment efficiency in the formulated NP are shown in table 4.26. NPs had mean particle size between $148.0 \pm 2.1\text{nm}$ and $169.9 \pm 6.3\text{nm}$.

Highest entrapment efficiency of $73.12 \pm 2.7\%$ could be obtained for batch no. EPPLUNP5. As the drug loading was increased from 9.0 to 14.2%, the entrapment efficiency increased, but at 20% drug loading the entrapment efficiency was decreased. This may be due to failure of the polymer to incorporate the excess of the drug in the nanoparticles (Quellec et al., 1998). Based on highest %EE and lowest mean particle size below 200nm, batch no. EPPLUNP5 was chosen to carry out stability and drug release study.

		Diam.(nm)	% Intensity	Width (nm)	
Z-Average (d.nm):	146	Peak 1:	167	100.0	64.9
Pdl:	0.117	Peak 2:	0.00	0.0	0.00
Intercept:	0.964	Peak 3:	0.00	0.0	0.00

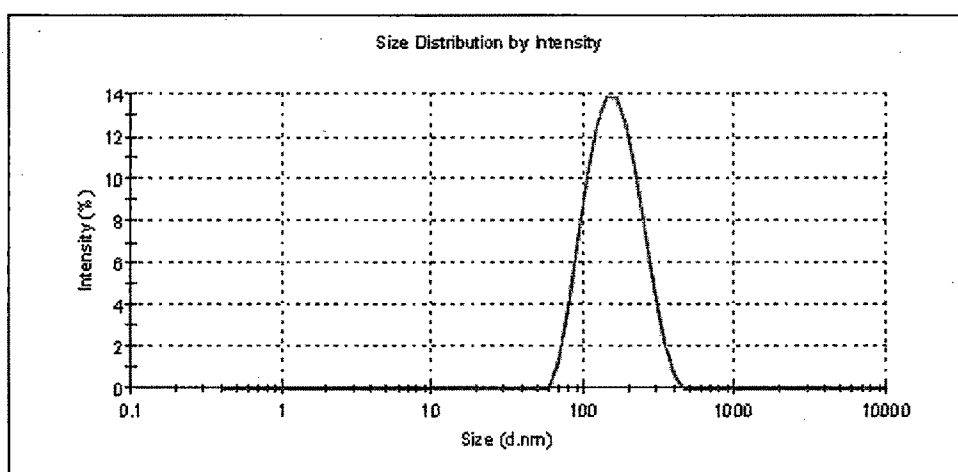


Fig. 4.28: Size distribution of ETO-PLGA-Pluronic NP

Fig 4.28 shows Size distribution of batch EPPLUNP5 with Mean particle size of 146.0nm. It was seen that the size distribution curve was bell shaped showing homogenous distribution of particles around the mean. This was also supported by a very low PDI of 0.117 indicating homogeneous particles.

Table 4.29
Batch details of Etoposide loaded PLGA-Pluronic NP and their MPS, Zeta potential and %EE

Batch No.	Drug :Polymer Ratio	Drug Loading %	Surf Conc. (% w/v)	MPS (nm) ± SD n=3	Zeta Potential (mV)	% EE ± SD n=3
EPPLU NP1	1:10	9.0	0.5	165.3 ±7.4	-17.1 ±1.3	54.21±2.3
EPPLU NP2	1:10	9.0	1.0	161.2 ±2.4	-18.6 ±2.0	53.27±3.42
EPPLU NP3	1:10	9.0	1.5	153.8 ±9.4	-19.2 ±1.4	52.09±3.13
EPPLUNP4	1:6	14.2	0.5	163.5 ±5.2	-17.2 ±1.6	65.20±1.4
EPPLUNP5	1:6	14.2	1.0	148.0 ±2.1	-20.0 ±1.2	73.12±2.7
EPPLU NP6	1:6	14.2	1.5	156.02 ±8.4	-21.2 ±2.0	71.22±1.1
EPPLU NP7	1:4	20.0	0.5	169.9 ±6.3	-18.7 ±0.7	65.50±1.4
EPPLU NP8	1:4	20.0	1.0	162.4 ±2.8	-19.8 ±2.3	64.21±2.4
EPPLU NP9	1:4	20.0	1.5	159.6 ±3.6	-21.5 ±1.6	63.11±3.2

4.13.5.1 Zeta potential of PLGA-PLURONIC NP

The measurement of zeta potential is a useful method for assessing the extent of coating on the surface of nanoparticles (Barratt, 1999). Nanoparticles prepared from PLGA-Pluronic copolymers were found to have negative zeta potential values ranging from $-17.1 \pm 1.3\text{mV}$ to $-21.5 \pm 1.6\text{mV}$ (Table 4.29). Fig 4.29 shows zeta potential distribution of batch EPPLUNP5. It was evident from that the graph that the nanoparticles had a narrow zeta deviation and a sharp peak was obtained at -20.0 mV . The high negative zeta values in the range of -15 mV to -30 mV keeps the NP stable (Kesisoglou et al., 2007). Hence the developed formulation which had zeta potential values in the same high negative region indicated stability of the NP.

	Mean (mV)	Area (%)	Width (mV)
Zeta Potential (mV): -20.0	Peak 1: -20.0	100.0	6.36
Zeta Deviation (mV): 6.36	Peak 2: 0.00	0.0	0.00
Conductivity (mS/cm): 0.0420	Peak 3: 0.00	0.0	0.00

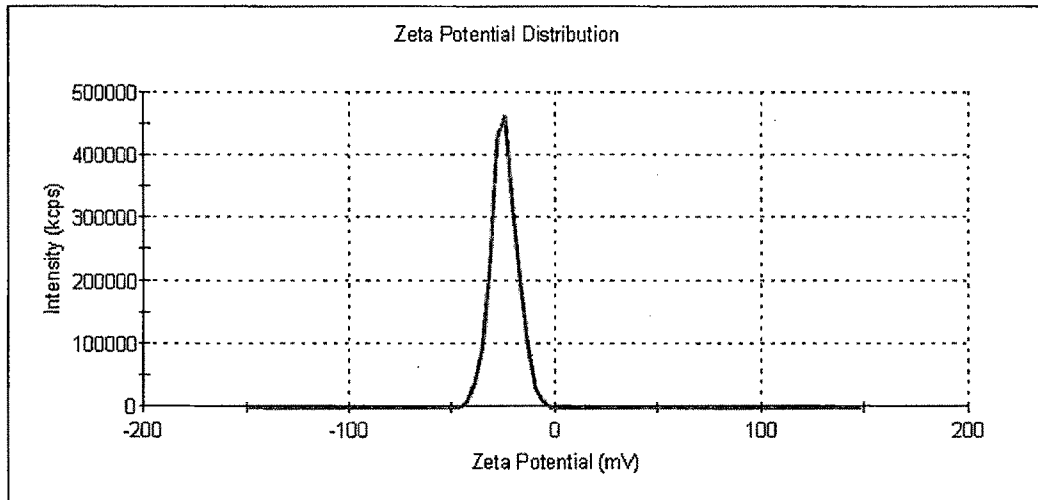


Fig. 4.29: Zeta potential of PLGA-Pluronic NP

The zeta potential of PLGA-Pluronic NP was comparatively reduced with respect to PLGA NP (-32.7mV). This decrease in zeta potential was attributed to Pluronic F-68 on the surface of the particle. The nanoparticles prepared with Poloxamer 188 have been reported to have low negative zeta potential but were sterically stable (Schwarz et al., 1994). It was concluded that the PLGA-Pluronic NP would be sterically stable.

4.13.6 Lyophilization and optimization of cryoprotectant

In the present study we used Sucrose and Trehalose in four concentrations of 10, 20, 50 and 100%w/w (Table 4.30). An increase in size of the NPs was seen following freeze-drying with the use of both cryoprotectants. Optimization of the cryoprotectant was based on its ability to give minimum increase in size and redispersibility. It was seen that use of sucrose in a 50%w/w concentration showed minimum increase in particle size for PLGA-mPEG NP. These NP were also having redispersibility. Use of 20% w/w sucrose showed minimum increase in particle size of PLGA-Pluronic NP after lyophilization. The dispersibility of these NP was good. The use of higher concentrations of cryoprotectants showed good dispersibility of the NP after lyophilization but had higher increase in MPS. The amount of Trehalose needed for dispersibility was very high (100% w/w) in both the NP and hence was not selected as the cryoprotectant.

Table 4.30
Optimization of Cryoprotectant for PLGA-mPEG NP and PLGA-Pluronic NP: Influence of lyophilization on Mean Particle Size (MPS) and redispersibility

Cryoprotectant	% w/w	PLGA-mPEG NP			PLGA-Pluronic NP		
		Mean particle Size (nm)		Redispersibility	Mean particle size (nm)		Redispersibility
		BL	AL		BL	AL	
No	0	95.1	124.4	ND	148.6	179.4	ND
	10	95.1	110.3	ND	148.6	163.4	ND
Sucrose	20	95.1	108.2	ND	148.6	161.2	D
	50	95.1	105.5	D	148.6	168.0	D
	100	95.1	107.3	D	148.6	175.4	D
	10	95.1	128.2	ND	148.6	169.2	ND
Trehalose	20	95.1	112.8	ND	148.6	167.0	ND
	50	95.1	108.1	ND	148.6	171.3	ND
	100	95.1	111.4	D	148.6	172.0	D

BL- Before Lyophilization, AL- After Lyophilization, D- dispersible, ND- non dispersible.

4.13.7 XRD studies

Figure 4.30 shows X-ray powder diffraction pattern of ETO, physical mixture (PM-ETO-PLGA-mPEG), PLGA-mPEG NP and PLGA-PLURONIC NP. ETO showed four principle peaks at 23°, 19°, 17° and 24°. In the physical mixture three peaks were visible at 23°, 25° and 19° though their intensities were reduced. It was observed that these characteristic peaks were absent in ETO loaded nanoparticles (PLGA-MPEG NP and PLGA-PLURONIC NP). Hence it could be concluded that in the prepared PLGA-mPEG and PLGA-Pluronic NP, the drug was present in the amorphous state and may have been homogeneously dispersed in the polymer matrix.

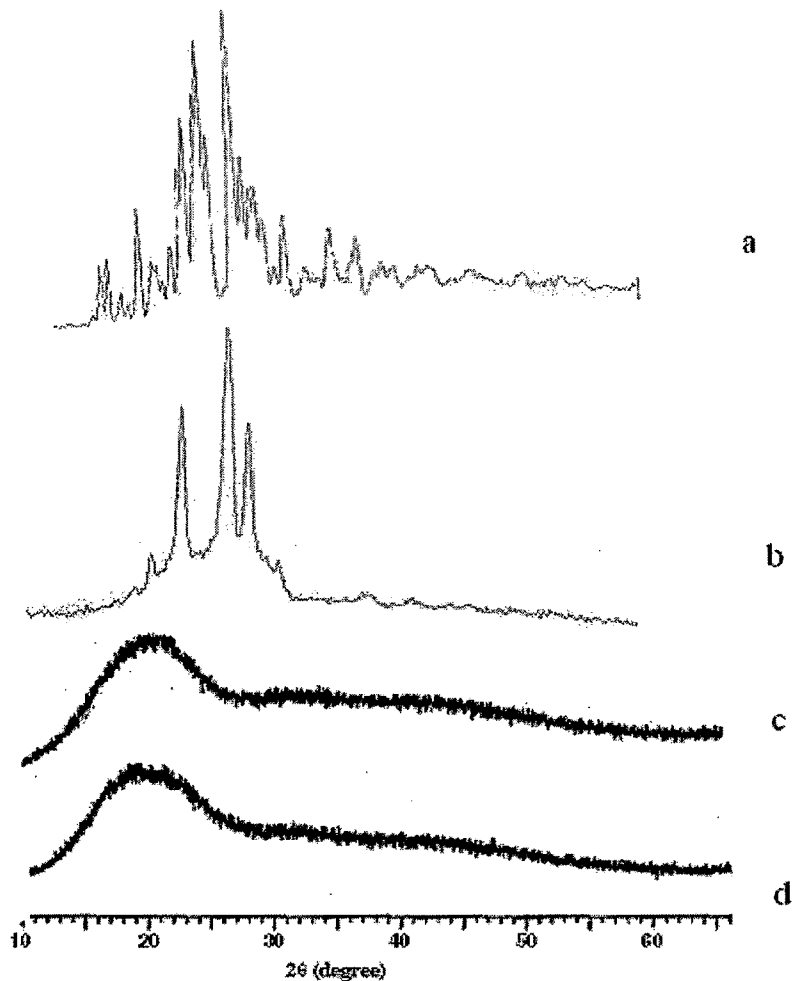


Fig. 4.30: XRD of (a) Etoposide, (b) Physical mixture of ETO-PLGA-mPEG, (c) Etoposide loaded PLGA-mPEG NP and (d) ETO loaded PLGA-Pluronic NP

4.13.8 SEM studies

The electron micrograph showed spherical discrete and homogenous particles in the nanometer size range (Fig. 4.31).

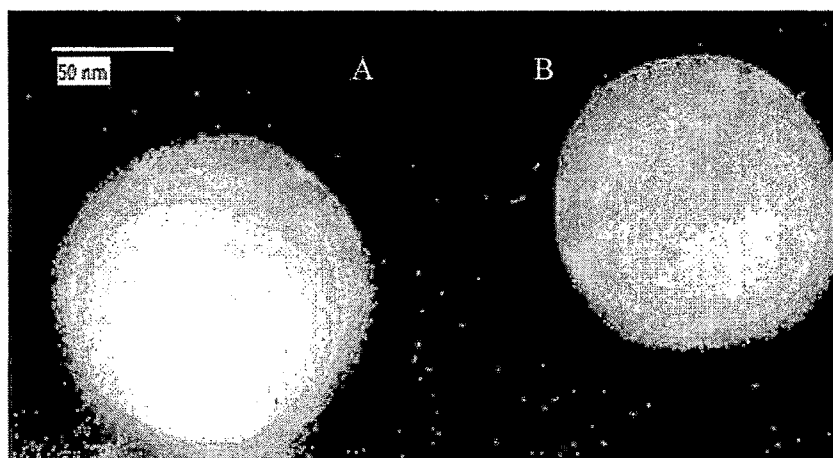


Fig. 4.31: SEM of Etoposide loaded PLGA-mPEG NP (A) and PLGA-Pluronic NP (B)

4.13.9 Drug Release studies

In vitro drug release from the pure drug was complete within 4 hours, but was sustained up to 7 days from PLGA-mPEG nanoparticles and 5 days from PLGA-Pluronic nanoparticles. The release profile is shown in Table 4.31 and Fig. 4.32.

In the first hour there was negligible drug release from both the NP formulations. It was seen that PLGA-mPEG Nanoparticles (EPMPEG NP) showed initial release of 26.6% in 12 h, whereas, EPPLU NP released 45.6% in 12h. Release from EPPLU NP was faster compared to EPMPEG NP. Less than 50% of the drug was released in 48 h from EPMPEG NP and around 75 % of the drug released from EPPLU NP in 48 h. The prolonged release may be attributed to the formation of a homogeneous matrix with the drug randomly distributed throughout the polymer. Two possible mechanisms may be involved in the release of drug from the PLGA based particles: the dissolution diffusion of drug from the matrices as well as the matrix erosion resulting from degradation of the polymers (Soppimath et al., 2001). Polymer degradation usually plays a crucial role in drug release from sustained release systems and PLGA is found to degrade in almost 120 days (Dunne et al., 2000). However, when the diffusion is faster than the matrix degradation the mechanism of drug release occurs mainly by diffusion (Niwa et al., 1993). Hence in our case the release was due to diffusion.

The release was first ordered and followed non-fickian diffusion kinetics in both the cases. Data fitted to Higuchi model (Fig 4.33) showed that EPMPEG NP had high r^2 value of 0.9929 indicated that it follows higuchi diffusion kinetics, where as EPPLU NP had a slightly low r^2 value of 0.945.

The release data were fitted using the well known empirical equation proposed by Korsmeyer and Peppas (Korsmeyer et al., 1983; Peppas, 1985)

$M_t/M_\infty = kt^n$. Where M_t/M_∞ is the accumulative release percent at time t, k is the kinetic constant incorporating structural and geometric characteristics of the release device, and n is the diffusional exponent indicative of the mechanism of drug release. The value of n for a spherical system is <0.43 for Fickian release, 0.43<n<0.85 indicates non-Fickian release, n> 0.85 indicates case II release (Siepmann and Peppas, 2001).

Table 4.31
In Vitro Drug Release Profile of Etoposide and Etoposide loaded Nanoparticles

Time (h)	% Drug Released (\pm SD)		
	ETO	EPmPEG NP	EPPLU NP
1	38.2 \pm 2.4	0.0 \pm 0.0	0.0 \pm 0.0
2	67.2 \pm 4.8	3.2 \pm 1.2	10.1 \pm 1.1
3	89.3 \pm 5.7	9.4 \pm 2.1	15.2 \pm 2.5
4	99.2 \pm 1.3	12.5 \pm 2.3	30.6 \pm 2.8
6		17.4 \pm 1.5	45.1 \pm 2.5
12		26.6 \pm 2.4	66.3 \pm 0.9
24		32.2 \pm 2.4	75.3 \pm 1.8
48		45.8 \pm 2.9	85.3 \pm 3.9
72		67.2 \pm 0.7	93.0 \pm 2.1
96		72.6 \pm 3.1	99.3 \pm 0.5
120		83.0 \pm 0.8	
144		93.4 \pm 0.6	
168		99.3 \pm 0.6	

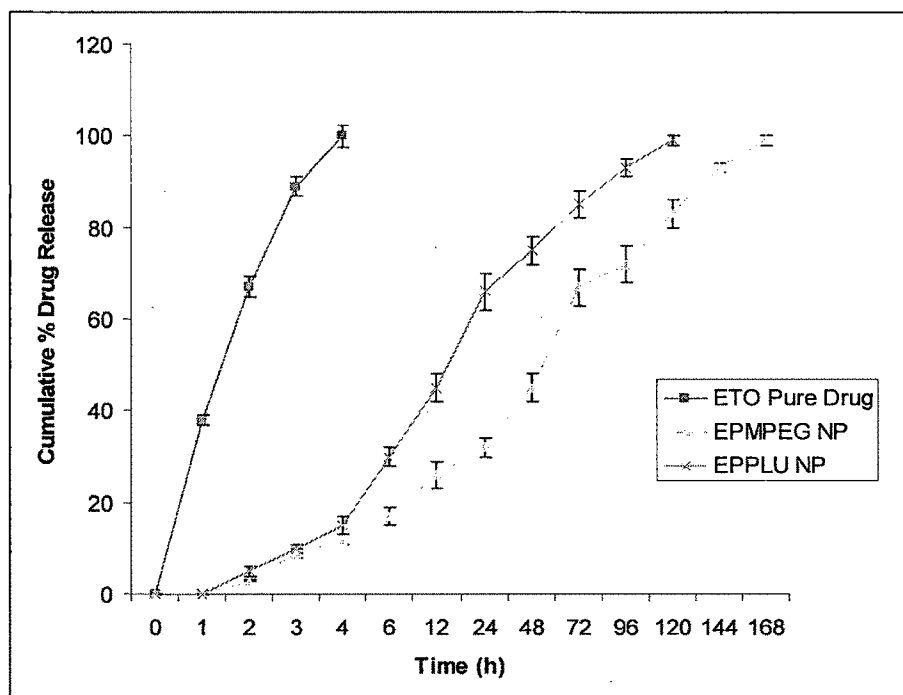


Fig. 4.32: In Vitro Drug Release Profile of Etoposide pure drug, Etoposide loaded PLGA-mPEG NP and Etoposide loaded PLGA-Pluronic Nanoparticles

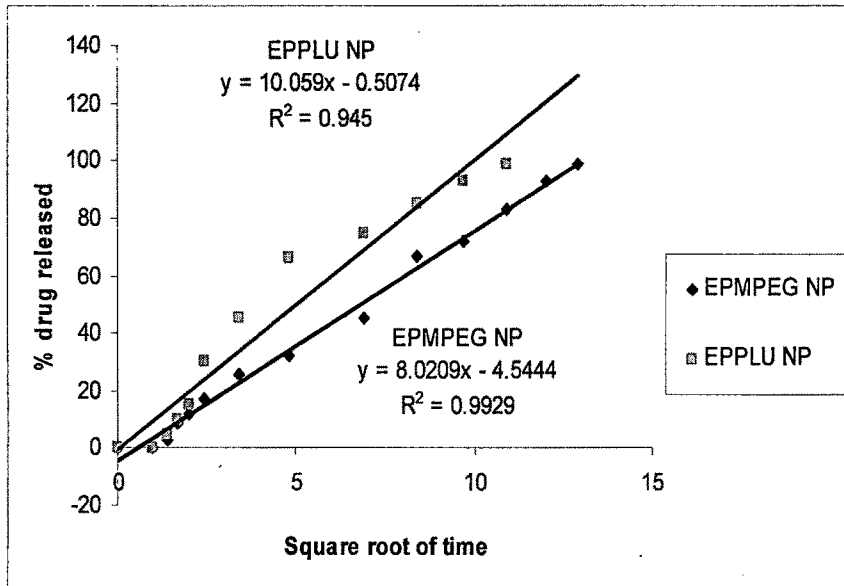


Fig 4.33: Drug Release Fitted to Higuchi Model

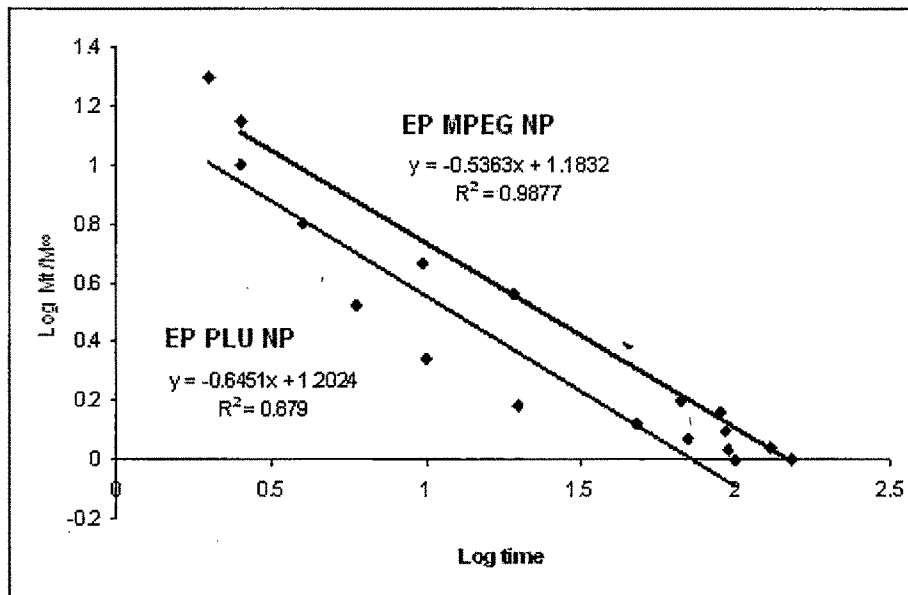


Fig 4.34: Korsmeyer-Peppas model for EPMPEG NP and EPPLU NP, $\text{Log } (M_t/M_\infty)$ is plotted against $\text{Log time } t$

Log (M_t/M_∞) is plotted against Log time t in the Korsmeyer-Peppas model shown in Fig. 4.34. The slope of the line gives the value of n , which indicated the release mechanism. For EPMPEG NP the n value was found to be 0.53 and for EPPLU NP the n value was found to be 0.64. both the values indicate a non-Fickian release. Table 4.32 gives the R^2 value of different models, values close to 0.98 indicate the type of model the release is fitting to. It was evident from the table that EPMPEG NP follows Higuchi, non-Fickian release, where as EPPLU NP does not follow Higuchi model but has non Fickian release kinetics.

Table 4.32
Drug release Kinetics
 R^2 values of zero, Higuchi, Korsmeyer-Peppas models and n value of Korsmeyer-Peppas model fitted to EPMPEG NP and EPPLU NP

Formulation	EPMPEG NP	EPPLU NP
Zero order	0.9501	0.9614
R^2 value		
Higuchi	0.9929	0.945
R^2 value		
Korsmeyer-Peppas,	0.9877	0.879
R^2 value		
Korsmeyer-Peppas,	0.53	0.64
n value		

It was concluded from the drug release studies that EPMPEG NP was able to sustain the release of etoposide up to 7 days and EPPLU NP was able to sustain the release for 5 days. The drug release from EPMPEG NP followed Higuchi diffusion kinetics and was non-Fickian. Whereas, EPPLU NP did not follow Higuchi model and had non-Fickian release kinetics.

4.13.10 Stability studies

Effect of Storage at 2-8°C on MPS

For Etoposide loaded PLGA-mPEG NP (EPMPEG NP) as well as Etoposide loaded PLGA-Pluronic NP (EPPLU NP) there was no significant change ($P>0.05$) in the mean particle size and in the % EE at 2-8°C for 1, 2 and 3 M in the FD state (Fig 4.35). Similarly there was no significant change ($P>0.05$) in the mean particle size of EPMPEG NP as well EPPLU NP at 2-8°C for 1M for AD. But there was a significant change in the mean particle size of both EPMPEG NP and EPPLU NP at 2-8°C for 2 and 3M for AD. The size of the particles increased significantly in the 3 months. The MPS of EPMPEG NP(AD) increased from initial 95nm to 99, 105 and 108 nm in 1, 2 and 3M respectively. The MPS of EPPLU NP(AD) increased from initial 151nm to 154, 158 and 161 nm in 1, 2 and 3M respectively.

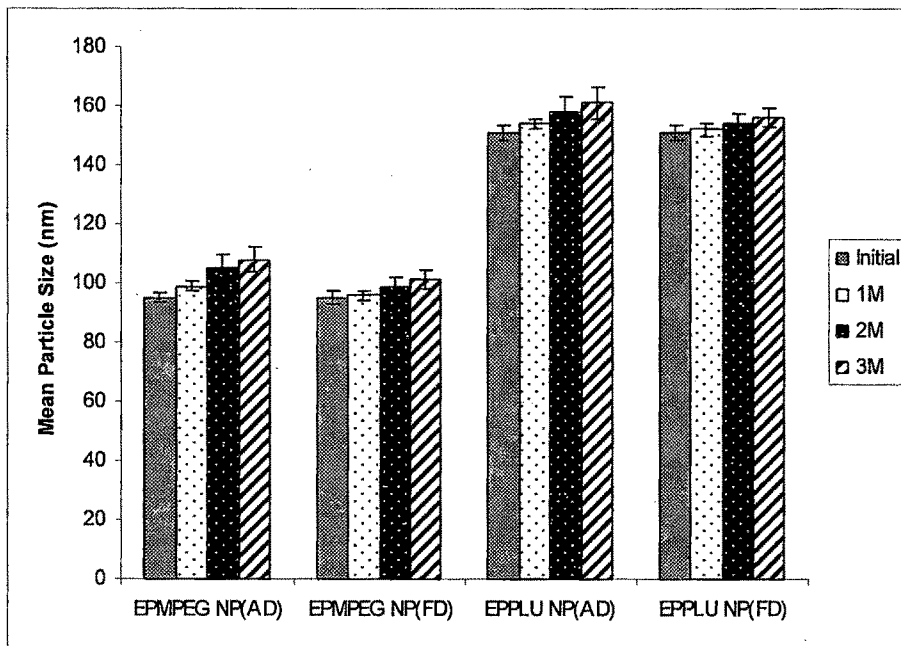


Fig. 4.35: Effect of storage at 2-8°C on Mean Particle Size of Etoposide loaded PLGA-mPEG NP (EPMPEG NP) and Etoposide loaded PLGA-Pluronic NP (EPPLU NP) in Aqueous Dispersion (AD) and Freeze Dried (FD). The values are mean of three batches with \pm S.D

Effect of storage at 25°C on MPS

For Etoposide loaded PLGA-mPEG NP (EPMPEG NP) as well as Etoposide loaded PLGA-Pluronic NP (EPPLU NP) there was no significant change ($P>0.05$) in the mean particle size at 25°C for 1M in both the FD and AD state (Fig 4.36). Similarly there was no significant change ($P>0.05$) in the mean particle size and % EE of EPMPEG NP as well EPPLU NP at 25°C for 1M in both the FD and AD.

But there was a significant change in the mean particle size and % EE of both EPMPEG NP and EPPLU NP at 25°C for 2 and 3M. The size of the particles increased significantly in the 3 months (Fig 4.32). The MPS of EPMPEG NP(AD) increased from initial 95nm to 107 and 112 nm in 2 and 3M respectively. The MPS of EPMPEG NP(FD) increased from initial 95nm to 101 and 105 nm in 2 and 3M respectively. The MPS of EPPLU NP(AD) increased from initial 151nm to 160 and 162 nm in 2 and 3M respectively. The MPS of EPPLU NP(FD) increased from initial 157nm and 159 nm in 2 and 3M respectively.

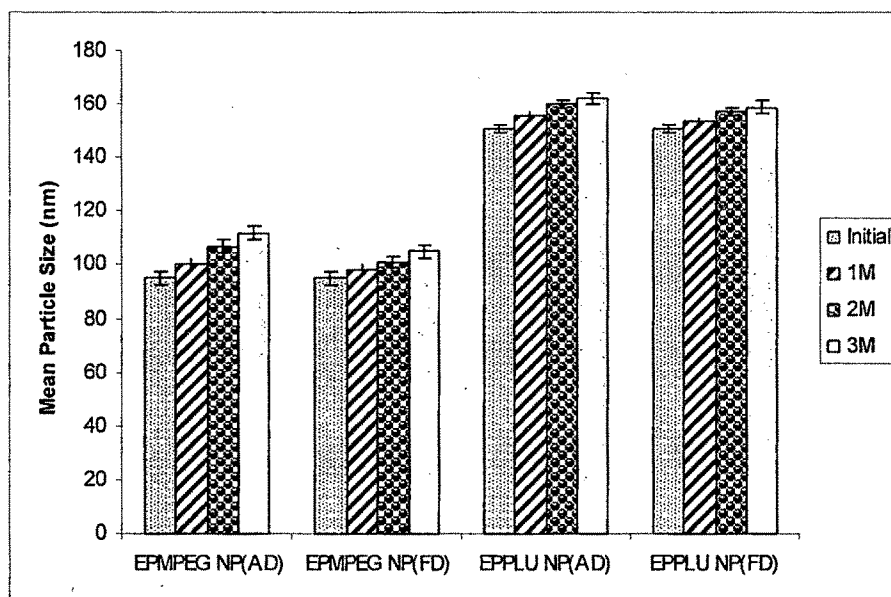


Fig. 4.36: Effect of storage at 25°C on Mean Particle Size of Etoposide loaded PLGA-mPEG NP (EPMPEG NP) and Etoposide loaded PLGA-Pluronic NP (EPPLU NP) in Aq. Dispersion (AD) and Freeze Dried (FD). The values are mean of three batches with \pm S.D

Effect of storage at 40°C on MPS

Etoposide loaded PLGA-mPEG NP (EPMPEG NP) as well as Etoposide loaded PLGA-Pluronic NP (EPPLU NP) were not stable at 40°C as there was significant change ($P>0.05$) in both the mean particle size and in the % EE (Fig 4.37). The MPS of EPMPEG NP(AD) increased from initial 95nm to 102, 109 and 115nm in the 1, 2 and 3M respectively. The MPS of EPMPEG NP(FD) increased from initial 95nm to 100, 103 and 109 nm in 1, 2 and 3M respectively. The MPS of EPPLU NP(AD) increased from initial 151nm to 158, 163 and 165 nm in 1, 2 and 3M respectively. The MPS of EPPLU NP(FD) increased from initial 151nm to 154, 156 and 161 nm in 1, 2 and 3M respectively.

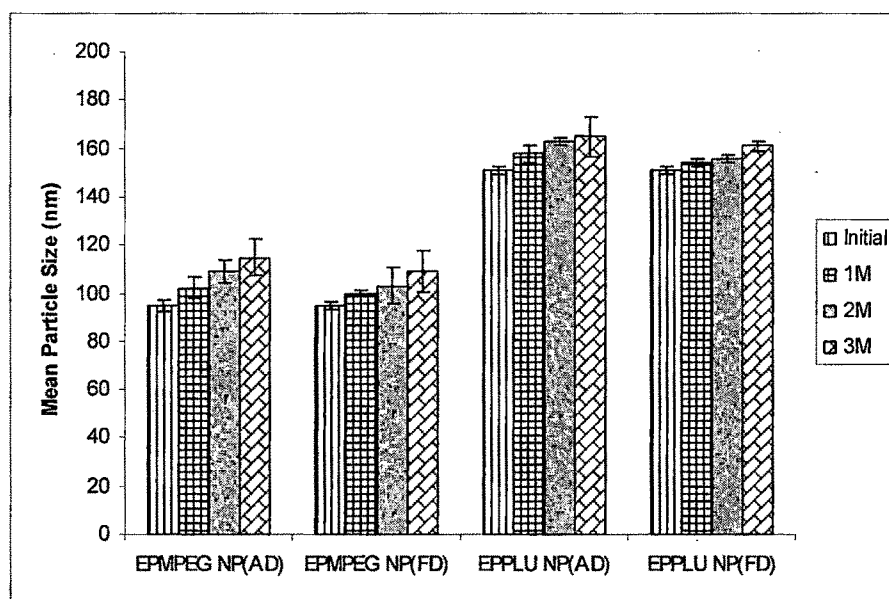


Fig. 4.37: Effect of storage at 40°C on Mean Particle Size of Etoposide loaded PLGA-mPEG NP (EPMPEG NP) and Etoposide loaded PLGA-Pluronic NP (EPPLU NP) in AD and FD states. The values are mean of three batches with \pm S.D

Conclusion

It was concluded from the stability studies that Etoposide loaded PLGA-mPEG NP (EPMPEG NP) and Etoposide loaded PLGA-Pluronic NP (EPPLU NP) were stable in terms of mean particle size at 2-8°C up to three months in the FD state, one month in the AD state at 2-8°C and for 1M in both the FD and AD state at 25°C. It has been reported that change in the mean particle size of nanoparticle happen over a period of time due to aggregation (Gasper MM et al, 1998). At higher temperature the NPs were not stable as an increase in size was observed.

Effect of storage at 2-8°C, 25°C and 40°C on drug content

EPMPEG NP (FD) did not show any significant change in the drug content in 1, 2 and 3M. EPMPEG NP (AD) did not show any significant change in the drug content ($P>0.05$) upto 2M, however, a significant change was observed in the 3M, where the drug content reduced to 92%. EPPLU NP (AD) and EPPLU NP(FD) at 2-8°C did not show any significant change ($P>0.05$) in the drug content in 1 and 2M. However, a significant change was observed for both in the 3rd month, where it was reduced to 90 and 92% respectively.

EPMPEG NP as well as EPPLU NP did not show any significant change ($P>0.05$) in the drug content at 25°C for 1M in both the AD and FD state (Fig 4.38 and 4.39). However, the drug content reduced to 94 and 95% for EPMPEG NP and 91 and 93% for EPPLU NP in the 2 and 3M for AD and FD state respectively.

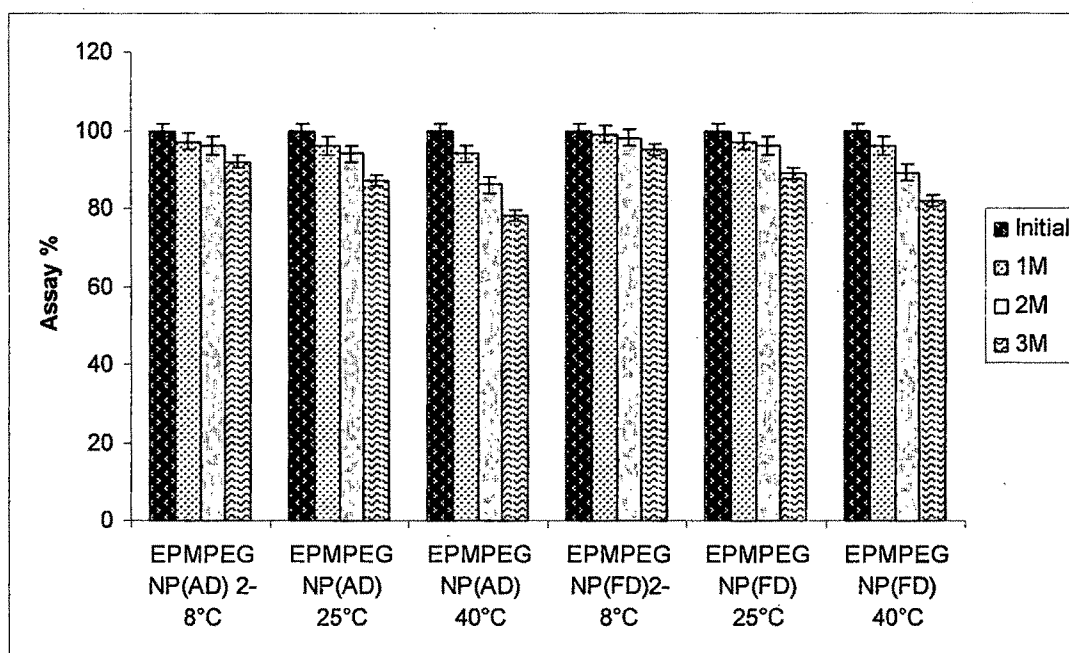


Fig. 4.38: Effect of storage at 2-8°C, 25°C and 40°C on Assay of Etoposide loaded PLGA-mPEG NP (EPMPEG NP) in AD and FD. The values are mean of three batches with \pm S.D

At 40°C, there was no significant change ($P>0.05$) in the assay in 1M for both EPMPEG NP and EPPLU NP in the FD states. However, the assay for FD states for both EPMPEG NP and EPPLU NP reduced to 89 and 82% for EPMPEG NP and 88, 78 for EPPLU NP in the 2 and 3M respectively.

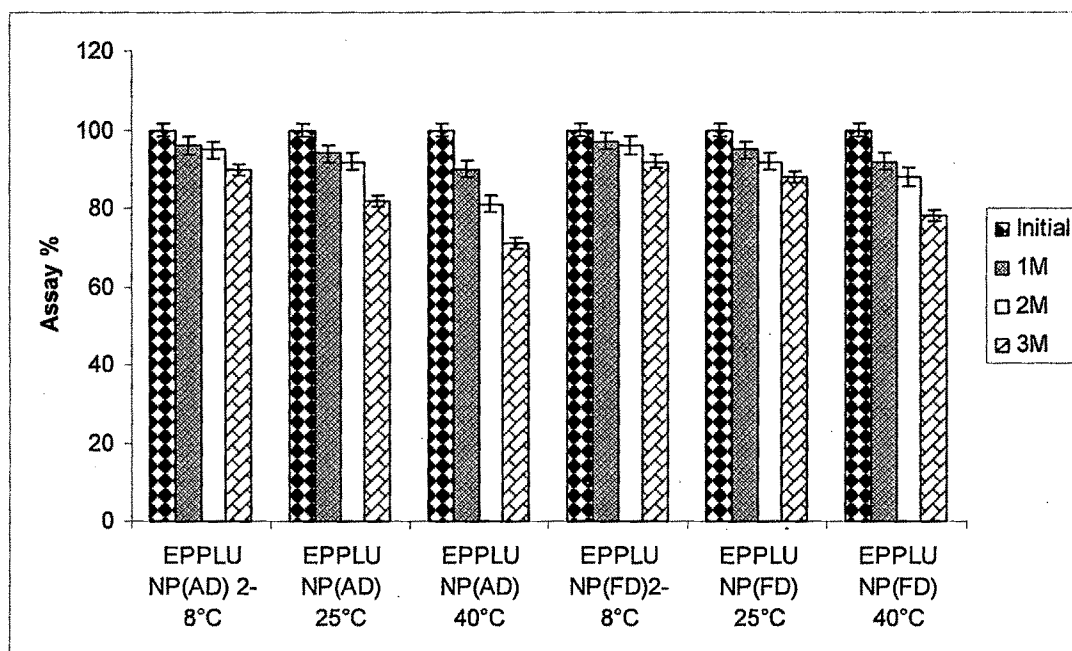


Fig. 4.39: Effect of storage condition at 2-8°C, 25°C and 40°C on Assay of Etoposide loaded PLGA-Pluronic NP (EPPLU NP) in Aqueous Dispersion (AD) and Freeze Dried (FD). The values are mean of three batches with \pm S.D

The drug content for EPMPEG NP(AD) decreased to 94, 86 and 78% in the 1, 2 and 3M respectively. The drug content for EPPLU NP(AD) reduced to 90, 81 and 71% in the 1, 2 and 3M respectively. The instability of NP at 40°C was due to particle aggregation and polymer degradation. The rate of polymer degradation has been found to increase with increasing temperature usually above 25°C (Dunne et al., 2000). The Polymer degradation releases the entrapped drug and thereby affects the drug content of the NP.

Conclusion

It was seen from the stability studies that Etoposide loaded PLGA-mPEG NP (EPMPEG NP) and Etoposide loaded PLGA-Pluronic NP (EPPLU NP) were stable in terms of % drug content upto three months in the FD state, two months in the AD state at 2-8°C, for 1M in both the FD and AD state 25°C and 1M in FD state at 40°C.

It was concluded that it is best to store nanoparticle formations in the freeze dried state at 2-8°C where it remains stable in terms of both MPS and drug content.

REFERENCES

- Ahlin P, Kristl J, Kristl A, Vrečer F (2002). Investigation of polymeric nanoparticles as carriers of enalaprilat for oral administration. *International Journal of Pharmaceutics* 239, 113–120.
- Avgoustakis K, Beletsi A, Panagi Z (2003). Effect of copolymer composition on the physicochemical characteristics, in vitro stability, and biodistribution of PLGA–mPEG nanoparticles. *International Journal of Pharmaceutics* 259, 115-127.
- Beletsi A, Leondiadis, Klepetsanis P, Ithakissios DS, Avgoustakis K (1999). Effect of preparative variables on the properties of PLGA–mPEG copolymers related to their application in controlled drug delivery. *International Journal of Pharmaceutics* 182, 187-197.
- Box G, Hunter W, Hunter J (1978). *Statistics for Experimenters: An Introduction to Design, Data Analysis and Model Building*. Wiley, New York.
- Brigger I, Dubernet C, Couvreur P (2002.) Nanoparticles in cancer therapy and diagnosis. *Advanced Drug Delivery Reviews* 54, 631–651.
- Chacon M, Molpeceres J, Berges L, Guzman M, Aberturas MR (1999). Stability and freeze-drying of cyclosporine loaded poly(D,L- lactide- glycolide) carriers. *European Journal of Pharmaceutical Sciences* 8, 99–107.
- Chorny M, Fishbein I, Danenberg HD, Golomb G (2002). Lipophilic drug loaded nanospheres prepared by nanoprecipitation: effect of formulating variables on size, drug recovery and release kinetics. *Journal of Controlled Release* 83, 389–400.
- Cohen S, Yoshiaka T, Lucarelli M (1991). Controlled delivery system for proteins based on poly (lactic/glycolic acid) microspheres. *Pharmaceutical Research* 8, 713–720.
- Dillen K, Vandervoort J, Mooter GV, Verheyden L, Ludwig A (2004). Factorial design, physicochemical characterisation and activity of ciprofloxacin-PLGA nanoparticles *International Journal of Pharmaceutics* 275, 171-187.
- Dunne M, Corrigan OI, Ramtoola Z (2000). Influence of particle size and dissolution conditions on the degradation properties of polylactide-co-glycolide particles. *Biomaterials* 21, 1659-1668.
- Freitas C and Muller RH (1998). Spray-drying of solid lipid nanoparticles (SLNTM). *European Journal of Pharmaceutics and Biopharmaceutis* 46, 145-151.
- Gaspar MM, Blanco D, Cruz ME, Alonso MJ (1998). Formulation of Lasparaginase-loaded poly(lactide-co-glycolide) nanoparticles: influence of polymer properties on enzyme loading, activity and in vitro release. *Journal of Controlled Release* 52, 53-62.

Gref R, Minamitake Y, Peracchia MT, Trubetskoy V, Torchilin V, Langer R (1994). Biodegradable long-circulating polymeric nanospheres, *Science* 263, 1600–1603.

Henwood JM and Brogden RN (1990). Etoposide: A review of its pharmacodynamic and pharmacokinetic properties, and therapeutic potential in combination chemotherapy of cancer. *Drugs* 39, 438-90.

Heurtault B, Saulnier P, Pech B, Proust JE and Benoit JP (2003). Physico-chemical stability of colloidal lipid particles, *Biomaterials* 24, 4283-4300.

Hocking RR (1976). Analysis and selection of variables in linear regression. *Biometrics* 32, 1-49.

ICH guidelines (www.ich.org)

Illum L, Davis SS (1984). The organ uptake of intravenously administered colloidal particles can be altered using a non-ionic surfactant (Poloxamer 338). *FEBS Letters* 167, 79–82.

Kesisoglou F, Panmai S, Wu Y (2007). Nanosizing - Oral formulation development and biopharmaceutical evaluation. *Advanced Drug Delivery Reviews* 59, 631–644.

Konan YN, Cerny R, Favet J, Berton M, Gurny R, Allemann E (2003). Preparation and characterization of sterile sub-200nm meso-tetra(4-hydroxyphenyl)porphyrin-loaded nanoparticles for photodynamic therapy. *European Journal of Pharmaceutics and Biopharmaceutics* 55(1), 115–24.

Korsmeyer RW, Gurny R, Doelker E, Buri P, Peppas NA (1983). Mechanisms of solute release from porous hydrophilic polymers. *International Journal of Pharmaceutics* 15, 25-35.

Langer R. (1997). Tissue engineering: a new field and its challenges. *Pharmaceutical Research* 14, 840–841.

Leo E, Brina B, Forni F, Vandelli MA (2004). In vitro evaluation of PLA nanoparticles containing a lipophilic drug in water-soluble or insoluble form. *International Journal of Pharmaceutics* 278, 133–141.

Mainardes RM and Evangelista RC (2005). Praziquantel-loaded PLGA nanoparticles: preparation and characterization. *Journal of Microencapsulation* 22(1), 13–24

Mandal TK, Bostanian LA, Graves RA, Chapman SR, Womack I (2002). Development of Biodegradable Microcapsules as Carrier for Oral Controlled Delivery of Amifostine. *Drug Development and Industrial Pharmacy* 28(3), 339–344.

Martinez-Sancho C, Herrero-Vanrell R, Negro S (2004). Optimisation of aciclovir poly(d,l-lactide-co-glycolide) microspheres for intravitreal administration using a factorial design study. *International Journal of Pharmaceutics* 273, 45–56

McCarron PA, Woolfson AD, Keating SM (1999). Response surface methodology as a predictive tool for determining the effects of preparation conditions on the physicochemical properties of poly(isobutylcyanoacrylate) nanoparticles. *International Journal of Pharmaceutics* 193, 37–47.

Montgomery DC (2004). Design and analysis of experiments, John Wiley and sons, 392-426.

Niwa T, Takeuchi T, Hino, Kunou N, Kawashima Y (1993). Preparations of biodegradable nanospheres of water-soluble and insoluble drugs with d,l-lactide/glycolide copolymer by a novel spontaneous emulsification solvent diffusion method, and the drug release behavior. *Journal of Controlled Release* 25, 89–98.

Panyam J, Zhou W, Prabha S, Sahoo SK, and Labhasetwar V (2002). Rapid endo-lysosomal escape of poly(DL-lactide-co-glycolide) nanoparticles: implications for drug and gene delivery. *The FASEB Journal* 16, 1217–1226.

Park TG (1995). Degradation of poly (lactide-co-glycolide acid) microspheres: effect of copolymer composition. *Biomaterials* 16, 1123–1130.

Passerini N, Craig DQ (2002). Characterization of cyclosporine A loaded poly (D,L lactide-co-glycolide) microspheres using modulated temperature differential scanning calorimetry. *Journal of Pharmacy and Pharmacology*. 54, 913-919.

Peppas NA (1985). Analysis of Fickian and non-Fickian drug release from polymers. *Pharm. Acta. Helv.* 60, 110-11.

Radwan MA (1995). In vitro evaluation of polyisobutylcyanoacrylate nanoparticles as a controlled drug carrier for theophylline. *Drug Development and Industrial Pharmacy* 21, 2371–2375.

Schwarz C, Mehnert W, Lucks JS, Muller RH (1994). Solid lipid nanoparticles (SLN) for controlled drug delivery I. Production, characterization and sterilization. *Journal of Controlled Release* 30, 83–96.

Siepmann and Peppas NA (2001). Modeling of drug release from delivery systems based on hydroxypropyl methylcellulose (HPMC). *Advanced Drug Delivery Reviews* 48, 139–157.

Soppimath KS, Aminabhavi T, Kulkarni AR, Rudzinski WE (2001). Biodegradable polymeric nanoparticles as drug delivery devices. *Journal of Controlled Release* 70, 1–20.

Thode K, Muller RH, Kresse M (2000). Two-time window and multiangle photon correlation spectroscopy size and zeta potential analysis-highly sensitive rapid assay for dispersion stability. *Journal of Pharmaceutical Sciences* 89, 1317–1324.

Vandervoort J, Ludwig A (2002). Biocompatible stabilizers in the preparation of PLGA nanoparticles: a factorial design study. *International Journal of Pharmaceutics* 238, 77–92.

Weiss B, Schaefer UF, Zapp J, Lamprecht A, Stallmach A, Lehr CM (2006). Nanoparticles made of Fluorescence –Labelled Poly(L-lactide-co-glycolide): Preparation, Stability and Biocompatibility. *Journal of Nanosciences and Nanotechnology* 6, 3048-3056.

Yang A., Yang L, Liu W, Li Z, Xu H, Yang X (2006). Tumor necrosis factor alpha blocking peptide loaded PEG-PLGA nanoparticles: preparation and *in vitro* evaluation. *International Journal of Pharmaceutics*, doi:10.1016/j.ijpharm.2006.09.015

Yoo HS, Oh JE, Lee KH, Park TG (1999). Biodegradable nanoparticles containing PLGA conjugate for sustained release. *Pharmaceutical Research* 16, 1114-1118.